N71-33401

NASA CONTRACTOR REPORT

NASA CR-1855

NASA CR-1855

CASE FILE COPY

A MATHEMATICAL MODEL OF PHYSIOLOGICAL TEMPERATURE REGULATION IN MAN

by J. A. J. Stolwijk

Prepared by
YALE UNIVERSITY SCHOOL OF MEDICINE
New Haven, Conn. 06510

for

NATIONAL AERONAUTICS AND SPACE ADMINISTRATION • WASHINGTON, D. C. • AUGUST 1971

1. Report No. NASA CR-1855	2. Government Accession No.	3. Recipient's Catalog No.
4. Title and Subtitle A MATHEMATICAL MODEL OF PHYSIOLOGICAL TEMPERATURE REGULATION IN MAN		5. Report Date August 1971
		6. Performing Organization Code
7. Author(s) J. A. J. Stolwijk		8. Performing Organization Report No.
		10. Work Unit No. 914 50 93 73
9. Performing Organization Name and Address John B. Pierce Foundation Laboratory and Department of Epidemiology and Public Health, Yale University School of Medicine New Haven, Connecticut 06510		11. Contract or Grant No. NAS 9-9531
		13. Type of Report and Period Covered Contractor Report
12. Sponsoring Agency Name and Address National Aeronautics and Space Administration Washington, D. C. 20546		14. Sponsoring Agency Code

15. Supplementary Notes

16. Abstract

A dynamic mathematical model is presented of physiological regulation of body temperature in man. A total of 25 nodes is used to represent the thermal characteristics of the body, with four nodes each representing the head, trunk, arms, hands, legs and feet. The twenty-fifth node represents the central blood. Each node has the appropriate metabolic heat production, convective heat exchange with the central blood compartments, and conductive heat exchange with adjacent compartments. The outer nodes represent the skin and exchange heat with the environment via radiation, convection and evaporation. In the model the thermoregulatory system receives temperature signals from all compartments and after integration and processing the system causes appropriate commands to be sent to all appropriate compartments changing metabolic heat production, blood flow or the rate of sweat secretion. The model is presented in the form of a documented FORTRAN program. Simulations of experimental exposures to step changes in environmental temperature at rest and of 30 minute exercise bouts at 25, 50 and 75 percent of maximum aerobic capacity at different ambient temperatures are compared with actual results.

17. Key Words (Suggested by Author(s))	18. Distribution Statement
body temperature regulation mathematical model of thermoregulation simulation of temperature regulation at rest and in exercise	Unclassified - Unlimited

19. Security Classif. (of this report)	20. Security Classif. (of this page)	21. No. of Pages	22. Price*
Unclassified	Unclassified	83	$3.00

*For sale by the National Technical Information Service, Springfield, Virginia 22151

CONTENTS

TABLES

FIGURES

Introduction

The deep space environment is a very hostile one for lifé as it exists on earth. The protection of space travelers from this hostile environment is a challenge to biology and technology in which both disciplines are dealing in largely uncharted territory. Solutions require communication between these disciplines of unprecedented effectiveness. In technology, the analysis of the behaviour of complex systems is a well-developed technique which yields many benefits. An important benefit is the ability to simulate the behaviour of a complex system under almost any imaginable set of circumstances using mathematical models with great savings in time and expense. The accuracy of such models of technological systems can be very high since the characteristics of their components are well known, and the controlling systems have known structure and characteristics.

It is highly desirable to develop similar mathematical models of biological systems for obvious reasons: simulations of the biological responses to dynamically varying sets of environmental circumstances would allow savings in time and expense required for evaluating the effects of such environments. Another very attractive feature of mathematical models of biological systems is that they can be made to communicate with models of technical systems, and it thus becomes possible to simulate the combined system of man with his life support system.

There are serious difficulties in constructing mathematical models of biological systems. These difficulties rest in the complexity of biological systems with respect to the number of identifiable components, but they are especially due to a great deal of redundancy in the control systems. This redundancy results in control systems with many multiple control loops. In a multiple control loop system, it is hard to study the system by opening one or more control loops since one cannot be sure that there are no remaining loops and that a particular component under study is really isolated.

It is thus not surprising that a mathematical model of thermoregulation of man, such as is described in this report, is far from accounting completely for all thermoregulatory responses ever reported. It can, however, give reasonable estimates of dynamic thermophysiological responses to a variety of environmental conditions and rates of internal heat production. This report is intended to present the current status together with the experimental findings which form the basis of much of the structure of the current model.

Development of the Model

An early forerunner of the current model was described in 1966 (1). This forerunner was implemented on an analog computer, but as the definition of the model increased, it soon became preferable to express the model equations in Fortran so that the simulations could be carried out on a digital computer. As proposed for models of the respiratory system by Yamamoto and Raub (2), symbol tables and equations will be given in a Fortran notation.

Although in practice the two are very closely interwoven, we can conceptually distinguish two separate systems in thermoregulation: the control system and the controlled system. The controlled system is a representation of the body in the thermal characteristics of its different parts. Thermal stresses act on the controlled system and cause strains. These thermal changes are recognized by sensor mechanisms belonging to the control system and after integration the control system causes corrective actions which act to reduce the thermal strain.

The controlled system in the current model consists of six segments, each with four concentric layers. A central blood compartment exchanges heat with all other compartments via the convective heat transfer occurring with the blood flow to each compartment. Each of the twenty-five compartments is represented by a heat balance equation which accounts for conductive heat exchange with adjacent compartments, metabolic heat production, convective heat exchange with the central blood compartment and evaporative heat loss and heat exchange with the environment if the compartment is in direct contact with the environment.

The Controlled System

The controlled system is based on a man with a body weight of 74.1 kg and a surface area of 1.89 m^2. It consists of the head which is considered as a sphere, and cylinders representing the trunk, the arms, the hands, the legs and the feet. Both arms, hands, legs and feet are represented by one cylinder each. Table 1 gives a list of symbols used in the controlled system with their definition and dimension.

TABLE 1

LIST OF SYMBOLS USED IN THE CONTROLLED SYSTEM WITH DEFINITION AND DIMENSIONS

Symbol	Vector Length	Definition	Dimensions
C (N)	25	Heat capacitance of compartment N	kcal . $°C^{-1}$
T (N)	25	Temperature of N	°C
F (N)	25	Rate of change of temperature in N	°C . h^{-1}
HF (N)	25	Rate of heat flow into or from N	kcal . h^{-1}
TC (N)	24	Thermal conductance between N and N + 1	kcal . h^{-1} . $°C^{-1}$
TD (N)	24	Conductive heat transfer between N and N+1	kcal . h^{-1}
QB (N)	24	Basal metabolic heat production in N	kcal . h^{-1}
Q (N)	24	Total metabolic heat production in N	kcal . h^{-1}
EB (N)	24	Basal evaporative heat loss from N	kcal . h^{-1}
E (N)	24	Total evaporative heat loss from N	kcal . h^{-1}
BFB (N)	24	Basal effective blood flow to N	l . h^{-1}
BF (N)	24	Total effective blood flow to N	l . h^{-1}
BC (N)	24	Convective heat transfer between central blood and N	kcal . h^{-1}
HC (I)	6	Convective and conductive heat transfer coefficient for Segment I	kcal . m^{-2} . h^{-1} . $°C^{-1}$
S (I)	6	Surface area of Segment I	m^2
HR (I)	6	Radiant heat transfer coeff. for Segment I	kcal . m^{-2} . h^{-1} . $°C^{-1}$
H (I)	6	Total environmental heat transfer coeff. for Segment I	kcal . h^{-1} . $°C^{-1}$
V		Air velocity	m . sec^{-1}
TAIR		Effective environmental temperature	°C
RH		Relative humidity in environment	———
TIME		Elapsed time	h
PAIR		Vapor pressure in environment	mm Hg
ITIME		Elapsed time	min
INT		Interval between outputs	min
DT		Integration step	h
P (I)	10	Vapor pressure table from 5 - 50°C	mm Hg
EMAX (I)	6	Calc. max. rate of evaporative heat loss from Segment I	kcal . h^{-1}
WORK		Total metabolic rate required by exercise	kcal . h^{-1}
PSKIN (I)	6	Saturated water vapor pressure at skin temp.	mm Hg

A schematic representation of one segment is given in Figure 1, showing the interrelations between the four concentric layers. The subscript I in Table 1 and hereafter refers to the segment, I = 1 being the head, I = 2 the trunk, I = 3 the arms, I = 4 the hands, I = 5 the legs and I = 6 the feet. The subscript N is used to indicate the individual compartments, such that N = $4^* I - 3$ always identifies the core layer of segment I, with N = $4^* I - 2$ representing the muscle layer, N = $4^* I - 1$ the subcutaneous fat layer and N = $4^* I$ is the skin compartment of segment I. The central blood compartment is represented by N = 25.

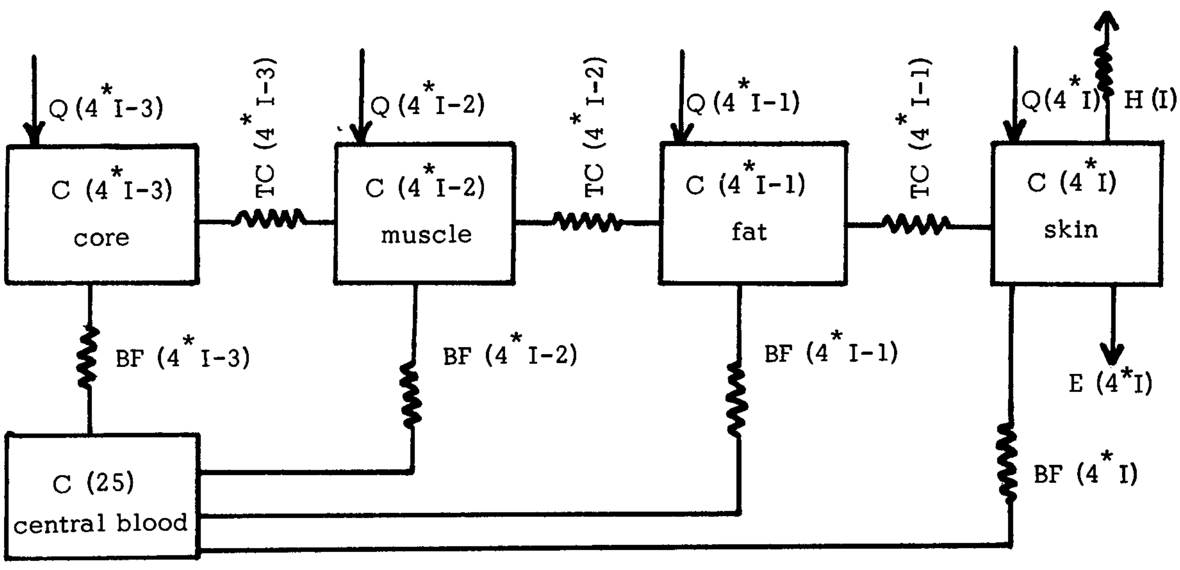

Figure 1. Schematic diagram of the four compartments of Segment I.

The first step in the development of the characteristics of the various segments is the determination of their relative surface areas and volume. Surface areas of men and women have been measured by many investigators, and Table 2 gives such values as selected from Meeh (3) and DuBois and DuBois (4) for men, and by Bradfield (5) for women as averages for 10 individuals each.

Table 2

Values for Surface Areas of Men and Women

Segment	Surface Area			
	10 men		10 women	
	m^2	% of total	m^2	% of total
Head	0.1326	7.00	0.1129	6.49
Trunk	0.6804	36.02	0.6279	36.07
Arms	0.2536	13.41	0.2210	12.70
Hands	0.0946	5.00	0.0783	4.50
Legs	0.5966	31.74	0.5904	33.92
Feet	0.1299	6.86	0.1100	6.32
TOTAL	1.8877	100.00	1.7404	100.00

Volume measurements of the various segments were not found in the literature in usable form, so that such measurements were approximated by measuring on five men and five women the circumference of the head, the length and two circumferences of the trunk, the length and circumference of the upper arm, and the length and two circumferences of the forearm. Similarly, the length of the thigh from crotch to knee, and two circumferences were measured for the thigh, and a similar set of measurements were taken for the lower legs; the volume of hands and feet were measured by displacement upon submersion in water. The volumes of the other segments were estimated from lengths and diameter assuming cylindrical shapes. The total estimated volumes were checked against the individual weights and were found to agree to within 8% with the total weight assuming a density of 1.00. Table 3 gives the percentages of the total volume in the various segments, as averaged for 5 men and 5 women.

Table 3

Percent of Total Body Volume in Six Segments

Segment	Men	Women	Average
Head	5.34	5.58	5.46
Trunk	56.70	57.00	56.85
Arms	7.78	6.52	7.15
Hands	0.88	0.90	0.89
Legs	27.90	28.70	28.30
Feet	1.43	1.34	1.38
TOTAL	100.00	100.00	100.00

According to Wilmer (6), the tissue distribution in the human body is 25% skin and fat, 11% viscera, nervous tissue 3%, muscle 43% and skeleton 18%.

Scammon (7) tabulates average weights of different body divisions and organs and his numbers can be used to make assignments of the tissue types to the layers in each segment as given in Table 4.

T a b l e 4

Distribution by weight of tissue types over the 4 layers in each of six segments as a percentage of total weight.

Segment	Skin	Fat	Muscle	Core				Total
	Skin	Tela subc	Muscle	Skeleton	Conn. Tissue	Viscera	Total	
Head	0.36	0.50	0.50	1.64	0.30	2.1	4.04	5.40
Trunk	1.81	9.50	24.09	3.80	4.00	11.9	19.70	55.10
Arms	0.65	1.30	4.53	2.02	1.00	--	3.02	9.50
Hands	0.25	0.20	0.10	0.31	0.04	--	0.34	0.90
Legs	1.61	3.20	13.68	6.73	2.58	--	9.31	27.80
Feet	0.32	0.30	0.10	0.50	0.08	--	0.58	1.30
TOTAL	5.00	15.00	43.00	15.00	8.00	14.0	37.00	100.00

With the aid of the preceding tables, the necessary computations to obtain C (N) and TC (N) can be carried out for any size man; but, for our purposes, we will limit ourselves to a "Standard" man with a height of 172 cm and a weight of 74.4 kg who, according to DuBois and DuBois (8) has a surface area of 1.89 m^2. The process for obtaining C (N) is indicated in Table 5. The values are based on a specific heat for the skeleton of 0.5 gcal/g . °C, 0.6 gcal/g . °C for fat and 0.9 gcal/g . °C for all other tissues. The central blood compartment representing the blood in the heart and the great vessels is assumed to contain 2.5 liters of blood at a specific heat of 0.9 gcal/g . °C. This heat capacitance of 2.25 Kcal/°C should be subtracted from the heat capacitance of the trunk core which thus becomes 9.82 Kcal/°C.

Thermal conductance between layers in each segment can be calculated from the dimensions derived before, using the method outlined by Stolwijk and Hardy (1). The lengths of the segments were obtained from measurements taken for the volume estimates described above. Results are given in Table 6. Although the volume estimates and surface area estimates have different origins, there is a considerable consistency in the data as can be demonstrated by recalculating the total surface area from the estimates in length and radius given in Table 6. Ignoring end surfaces, such a calculation yields a value very close to the DuBois area assumed at the outset.

Table 5

Weight and Specific Heat of the Four Layers in Each Segment

			Core						Muscle		Fat		Skin	
			Skeleton		Viscera, etc		Total							
Segment	% of total	Wt Kg	Wt Kg	C Kcal/°C	Wt Kg	C Kcal/°C	Wt Kg	C Kcal/°C	Wt Kg	C Kcal/°C	Wt Kg	C Kcal/°C	Wt Kg	C Kcal/°C
Head	5.4	4.02	1.22	0.61	1.79	1.61	3.01	2.22	0.37	0.33	0.37	0.22	0.27	0.24
Trunk	55.1	41.00	2.83	1.41	11.85	10.66	14.68	12.07	17.90	16.15	7.07	4.25	1.35	1.21
Arms	9.5	7.06	1.51	0.75	0.74	0.66	2.25	1.41	3.37	3.04	0.97	0.58	0.48	0.43
Hands	0.9	0.67	0.23	0.11	0.03	0.03	0.26	0.14	0.07	0.06	0.15	0.09	0.19	0.17
Legs	27.8	20.68	5.02	2.51	1.92	1.73	6.94	4.24	10.19	9.17	2.38	1.43	1.20	1.08
Feet	1.3	0.97	0.37	0.18	0.06	0.05	0.43	0.23	0.07	0.06	0.22	0.13	0.24	0.22
Total	100.0	74.40	11.18	5.57	16.39	14.74	27.57	20.31	31.97	28.81	11.16	6.70	3.73	3.35

Table 6

Calculation of Estimated Thermal Conductance Between Compartments

		Volume cm^3	Length cm	Radius cm	Avg. cond. gcal/cm . °C . sec x 10^4	TC (N) Kcal/°C . h
Head	core	3010	---	8.98	10	1.38
	muscle	3380	---	9.32	10	11.4
	fat	3750	---	9.65	8	13.8
	skin	4020	---	9.88	8	---
Trunk	core	14680	60	8.75	10	1.37
	muscle	32580	60	13.15	10	4.75
	fat	39650	60	14.40	8	19.80
	skin	41000	60	14.70	8	---
Arms	core	2240	112	2.83	10	1.20
	muscle	5610	112	4.48	10	8.90
	fat	6580	112	4.85	8	26.20
	skin	7060	112	5.02	8	---
Hands	core	260	96	0.93	10	5.50
	muscle	330	96	1.04	10	9.65
	fat	480	96	1.27	8	9.90
	skin	670	96	1.49	8	---
Legs	core	6910	160	3.71	10	9.0
	muscle	17100	160	5.85	10	12.4
	fat	19480	160	6.23	8	64.0
	skin	20680	160	6.42	8	---
Feet	core	430	125	1.06	10	14.0
	muscle	510	125	1.14	10	17.7
	fat	730	125	1.36	8	14.1
	skin	970	125	1.57	8	---

The various segments have different dimensional characteristics and, as a result, the overall environmental heat transfer coefficient H (I) has different values. Radiant heat transfer depends on effective radiant surface areas which are high for head and trunk, somewhat lower for arms and legs and even lower for hands and feet. Estimates for the effective radiant heat transfer coefficients of the six segments are given in Table 7. It should be pointed out that these are estimates, and that behavioral adjustments can increase and decrease these coefficients substantially. The values for the convective heat transfer coefficient given in Table 7 are based on measurements by Nishi and Gagge (9) in our laboratory using the naphthalene mass transfer method. They represent values in still air and we can assume that the effective air speed was 0.1 m . sec^{-1} due to gravitational convection. The combined heat transfer coefficient H (I) can be calculated for any air speed V by the expression

$$H (I) = (HR (I) + HC (I)^{*} (V/0.1)^{**} 0.5)^{*} S (I)$$

This expression is valid within about ± 5% for an ambient temperature range of 10° to 40°C and for air velocities up to 10 m . sec^{-1}.

The value for the combined heat transfer coefficient is slightly higher than found experimentally for sitting, resting subjects in shorts (10, 11), but this could be due to the minimal clothing and to behavioral adjustments of their effective surface area by the subjects.

Table 7

Estimated and Calculated Combined Environmental Heat Transfer Coefficient for a Nude Man Standing in a Thermally Uniform Environment

Segment	Shape	Length cm	Radius cm	Radiant heat transfer coeff. $Kcal.m^{-2}.h^{-1}.°C^{-1}$ HR (I)	Convective heat transfer coeff. ($v = 0.1\ m\ .\ sec^{-1}$) $Kcal.m^{-2}.h^{-1}.°C^{-1}$ HC (I)	Combined coefficient $Kcal\ .\ m^{-2}\ .\ h^{-1}\ .\ °C^{-1}$
Head	Sphere	--	9.88	5.5	2.75	8.25
Trunk	Cylinder	60	14.70	4.5	2.15	6.65
Arms	Cylinder	112	5.02	4.3	3.0	7.30
Hands	Cylinder	96	1.49	3.0	3.35	6.35
Legs	Cylinder	160	6.42	4.0	2.75	6.75
Feet	Cylinder	125	1.57	4.0	3.0	7.0

The model will be called upon to compute heat loss caused by evaporation of secreted sweat. The amount of sweat secreted is determined by the controlling system. For any given set of conditions there is a maximum rate of evaporation which is possible, indicated by EMAX (I) for segment (I). This maximum rate depends on the vapor pressure in air PAIR, the vapor pressure at the skin PSKIN (I) and the convective heat transfer coefficient H (I) - HR (I)* S(I). The following expression will compute EMAX (I) for segment I:

EMAX (I) = (PSKIN (I) - PAIR)* 2.2 * (H (I) - HR (I) * S (I))

in which 2.2 is the Lewis relationship as described and validated by Brebner, et al. (12). If E (4 * I) for any segment I exceeds EMAX (I), then it must be reduced to EMAX (I). The ratio E (4 * I) / EMAX (I) for each segment gives the fractional wetted area, a factor first described by Gagge (13) and later implicated as an important determinant in thermal comfort by Gagge, et al. (14). A weighted average of this ratio will correspond to the wetted area described in these reports.

Aschoff and Wever (15) have estimated that the metabolic rate of the brain is 16% of the total basal metabolic rate, and that the trunk core accounts for 56% of the resting metabolic rate. They estimate the total skin and musculature to produce 18% of the basal metabolic heat which leaves 10% for the skeleton and connective tissue. If the resting metabolic rate is presumed to be 74.4 Kcal . h^{-1} for the whole standard man (39.4 Kcal . m^{-2} . h^{-1}), the head core has a metabolic rate of 11.9 Kcal . h^{-1}, and the trunk core of 41.6 Kcal . h^{-1}. A total resting metabolic rate of 13.4 Kcal . h^{-1} is to be divided between skin and musculature. If the resting metabolic rate is 0.3 Kcal . h^{-1} . kg^{-1} for skin tissue and subcutaneous fat is included in this, we find a total of 4.47 Kcal . h^{-1} to be divided between the various skin and fat layers. This leaves 8.93 Kcal . h^{-1} to be divided proportionally between the different muscle compartments. All core compartments can then share the remainder of the resting heat production in proportion to their weight. The values of $\dot{Q}B$ (N) resulting from these estimates and considerations are given in Table 8.

In the resting state, the total evaporative heat loss is about 18 Kcal . h^{-1} (Stolwijk and Hardy (10)). Of this, about half, or 9 Kcal . h^{-1} represents respiratory heat loss which is considered to come from the trunk core. The remaining 9 Kcal . h^{-1} comes from the skin and represents diffusion losses through the skin. Strictly speaking both of these values are affected to some extent by the water vapor pressure in the ambient air, but this effect is relatively small and is ignored for our present purposes.

The values of basal evaporative heat loss EB (N) resulting from these estimates are given in Table 8.

The controlled system is further characterized by convective heat exchange between its parts as a result of blood flow. Certain regions are characterized by a very constant blood flow. The brain receives a very constant flow of about 750 ml . mm^{-1} or 45 l . h^{-1} (16). Resting muscle can be assumed to require 1.2 l . h^{-1} of blood flow for each Kcal . h^{-1} of metabolic heat production, purely on the basis of supplying the needed oxygen. Stolwijk and Hardy (1) added up the blood flows to visceral organs in the trunk core and estimated a total flow of 210 l . h^{-1}. The skin, in the resting state, receives far more blood flow than is required to sustain its metabolic rate. Behnke and Willmon (17) found a total skin blood flow in resting man of 240 ml . mm^{-1} . m^{-2} at an ambient temperature of 35°C which would cause considerable vasodilatation. In the neutral environmental temperature of 30°C, this is assumed to be reduced to 105 ml . min^{-1} . m^{-2} in proportion to the reduction in core to skin conductance which occurs at an environmental temperature of 30°C in comparison with 35°C. Hertzman, et al. (18) investigated the distribution of blood flow to different skin areas, and skin blood flow was distributed in Table 8 according to his findings.

Table 8
Estimate of Core Compartment Resting State Heat Production and Basal Evaporative Heat Losses

Segment (I)	Layer	(N)	Weight kg	C (N)	QB (N)	EB (N)	BFB (N)
Head (1)	core	1	3.01	2.22	12.84	---	45.00
	muscle	2	0.37	0.33	0.10	---	0.12
	fat	3	0.37	0.22	0.11	---	0.13
	skin	4	0.27	0.24	0.08	0.63	1.44
Trunk (2)	core	5	12.18	9.82	45.38	9.00	210.00
	muscle	6	17.90	16.15	5.00	---	6.00
	fat	7	7.07	4.25	2.13	---	2.56
	skin	8	1.35	1.21	0.40	3.25	2.10
Arms (3)	core	9	2.25	1.41	0.70	---	0.84
	muscle	10	3.37	3.04	0.95	---	1.14
	fat	11	0.97	0.58	0.17	---	0.20
	skin	12	0.48	0.43	0.13	1.20	0.50
Hands (4)	core	13	0.26	0.14	0.08	---	0.10
	muscle	14	0.07	0.06	0.20	---	0.24
	fat	15	0.15	0.09	0.03	---	0.04
	skin	16	0.19	0.17	0.05	0.45	2.00
Legs (5)	core	17	6.94	4.24	2.23	---	2.69
	muscle	18	10.19	9.17	2.86	---	3.43
	fat	19	2.38	1.43	0.43	---	0.52
	skin	20	1.20	1.08	0.32	2.85	2.85
Feet (6)	core	21	0.43	0.23	0.13	---	0.16
	muscle	22	0.07	0.06	0.02	---	0.02
	fat	23	0.22	0.13	0.04	---	0.05
	skin	24	0.24	0.22	0.07	0.62	3.00
	Central Blood	25	2.50	2.25	---	---	---
Total			74.45	59.17	74.45	18.00	285.13

The Controlling System

The controlling system in body temperature regulation can be divided into three distinctly separate parts. The first part contains the sensing mechanisms which recognize the thermal state of the controlled system. The second part receives information regarding the thermal state, integrates it and sends out appropriate effector commands to the various effector systems. The third part of the controlling system receives the effector commands and if appropriate modifies them according to the conditions at the periphery before translating such commands into effector action.

Thermoreceptors have been described in a wide variety of locations in the body. Sometimes these descriptions are based on functional thermosensitivity in short, local temperature changes and produce thermoregulatory effector output much in excess of the size of the stimulus. On other occasions, and using electrophysiological methods, investigators find fibers in which the electrical activity is determined by the temperature of tissues innervated by such a fiber.

Areas in which thermosensitivity has been demonstrated by both methods are the preoptic area and anterior hypothalamus in the brain (19, 20), the spinal cord (21, 22) and the skin (23, 24), and the abdominal viscera (25, 26). Other areas have been suspected, such as muscle tissue or the veins draining muscle (27). Final and irrefutable proof of the functional role of thermosensitive areas, and the precise mode of detection is extremely difficult to obtain, even for the anterior hypothalamic area where there is general acceptance of the importance in thermoregulation.

Such uncertainties stem from the fact that it is usually difficult to dissociate temperatures in various parts of the body because of the strong thermal coupling which takes place. Uncoupling for experimental purposes is difficult because it can only be achieved for a very short time during rapid transients in load. During such transients, thermal fluxes are high, thermal gradients are steep, and the available time is short, all adding up to potential errors in such measurements and to general difficulties in devising appropriate methods.

A listing of all symbols used in the description of the controlling system is given in Tables 9 and 10.

In order to allow for maximum flexibility in the evaluation of different thermoregulatory controller concepts, it is easiest to assume that thermoreceptor structures are present in all tissues. Error signals are derived from all compartments with the following expression:

$$\text{ERROR (N)} = \text{T (N)} - \text{TSET (N)} + \text{RATE (N)}^{*}\ \text{F (N)}$$

In first approximation, the error signal is thus equal to the difference between the instantaneous temperature T (N) and the reference temperature TSET (N). For appropriate compartments where dynamic sensitivity of the thermoreceptors is quantitatively known, the dynamic term RATE (N)* F (N) can assume non-zero values. T (N) and F (N) are continuously computed from the passive system, and TSET (N) and RATE (N) are controlling system characteristics supplied as initial constants.

T a b l e 9

Definition of Symbols Used in the Description of the Controlling System

Symbol	Vector Length	D e f i n i t i o n	Dimension
TSET (N)	25	"Set point" or reference point for receptors in compartment N	°C
ERROR (N)	25	Output from thermoreceptors in compartment N	°C
RATE (N)	25	Dynamic sensitivity of thermoreceptors in N	h
COLD (N)	25	Output from cold receptors in N	°C
WARM (N)	25	Output from warm receptors in N	°C
COLDS		Integrated output from skin cold receptors	°C
WARMS		Integrated output from skin warm receptors	°C
SWEAT		Total efferent sweat command	Kcal . h^{-1}
CHILL		Total efferent shivering command	Kcal . h^{-1}
DILAT		Total efferent skin vasodilation command	l . h^{-1}
STRIC		Total efferent skin vasoconstriction command	N. D.
SKINR (I)	6	Fraction of all skin receptors in Segment I	N. D.
SKINS (I)	6	Fraction of sweating command applicable to skin of Segment I	N. D.
SKINV (I)	6	Fraction of vasodilatation command applicable to skin of Segment I	N. D.
SKINC (I)	6	Fraction of vasoconstriction command applicable to skin of Segment I	N. D.
MWORK (I)	6	Fraction of total work done by muscles in Segment I	N. D.
MCHIL (I)	6	Fraction of total shivering occurring in muscles of Segment I	N. D.

Table 10

Definition of Symbols Used as Control Coefficients

Symbol	Definition	Dimension
CSW	Sweating from head core	$Kcal \cdot h^{-1} \cdot {}^{\circ}C^{-1}$
SSW	Sweating from skin	$Kcal \cdot h^{-1} \cdot {}^{\circ}C^{-1}$
CDIL	Vasodilatation from head core	$l \cdot h^{-1} \cdot {}^{\circ}C^{-1}$
SDIL	Vasodilatation from skin	$l \cdot h^{-1} \cdot {}^{\circ}C^{-1}$
CCON	Vasoconstriction from head core	${}^{\circ}C^{-1}$
SCON	Vasoconstriction from skin	${}^{\circ}C^{-1}$
CCHIL	Shivering from head core	$Kcal \cdot h^{-1} \cdot {}^{\circ}C^{-1}$
SCHIL	Shivering from skin	$Kcal \cdot h^{-1} \cdot {}^{\circ}C^{-1}$
PSW	Sweating from skin and head core	$Kcal \cdot h^{-1} \cdot {}^{\circ}C^{-2}$
PDIL	Vasodilatation from skin and head core	$l \cdot h^{-1} \cdot {}^{\circ}C^{-2}$
PCON	Vasoconstriction from skin and head core	${}^{\circ}C^{-2}$
PCHIL	Shivering from skin and head core	${}^{\circ}C^{-2}$
BULL	Factor determining temperature sensitivity of sweat gland response	${}^{\circ}C^{-1}$

There can be conceptual controllers (1, 21) which are based on outputs which have a positive value on one side of the reference point, and have no output on the other side of the set point. This conceptual construction is supported by the obvious fact that there can be no negative firing rate, or negative sweating, negative blood flow or negative shivering. Non-linearity is thus introduced somewhere in the chain from receptors to effectors, and it is convenient to have this non-linearity available at the receptor level. This is conveniently accomplished by testing ERROR (N) for its sign. If it is positive, we can assume warm receptors are active, and WARM (N) can be set to the value of ERROR (N). If ERROR (N) is negative, we are dealing with a cold receptor output, and COLD (N) can be set to -ERROR (N). The resulting lists of WARM (N), COLD (N) and ERROR (N) then contain all thermal information which could be available to the thermoregulatory controller. There is very little information concerning the distribution of receptors in different compartments. This is of special importance in tissues which are widespread so that different compartments can be at widely different temperatures. The skin is a prime example. In the absence of any further information, the simplest approach would be the weight of the different compartments in different segments according to their mass. For the skin, Aschoff and Wever (15) have proposed relative sensitivities which can be adopted although their factual basis is not clear. Bader and Macht (28) show a relatively higher sensitivity in the skin of head and chest than in the extremities, but there is reason to suspect that in their case the heat applied to the skin was sufficient to warm the central blood appreciably so that deeper or central thermoreceptors could have been involved in producing the results they observed.

There is little doubt that the trunk skin plays a more than proportionate role in skin thermoreception as evidenced by the difference in response to a uniform skin temperature and to an identical average skin temperature with divergent local temperatures. The tentative values for SKINR (I) shown in Table 11 have been obtained by multiplying the number of cold points for various segments given by Aschoff and Wever (15) with the corresponding surface areas and assigning to each area the appropriate fraction of the total sum of these products.

Hertzman and Randall (18) surveyed the skin with respect to local blood flow. Although their measurements were photoelectric and consequently hard to quantitate, the relative proportions can probably be accepted. After rearrangement, the following fractions of the total blood flow are obtained for the basal and maximally dilated state respectively: head 0.288 and 0.132, trunk 0.265 and 0.322, arms 0.078 and 0.095, hands 0.10 and 0.122, legs 0.186 and 0.23, and feet 0.083 and 0.10.

The fractions for the maximally dilated state are taken as the distribution of vasodilatation over the skin, SKINV (I), in Table 11. Vasoconstriction is also not uniform over the skin area. In addition, the effects of countercurrent heat exchange will tend to exaggerate the effects of vasoconstriction in the distal extremities. On the other hand, countercurrent heat exchange is not so pronounced in the skin of the head and the trunk. Based on this, the assignments of SKINC (I) are made as shown in Table 11.

The relative distribution of sweat secretion in the absence of information based on local secretion measurements is perhaps best approximated by the distribution of sweat glands. Randall (29) made such observations and the different skin areas were weighted as to the number of sweat glands, and the fractional distribution is given as SKINS (I) in Table 11. In addition, some weight was given to provisional results from thermograms presented by Stolwijk, et al. (30).

Table 11

Tentative Estimates of Distribution of Sensory Input and Effector Output Over the Various Skin Areas

Segment	Surface Area m^2	Surface Area %	SKINR (I)	SKINS (I)	SKINV (I)	SKINC (I)
Head	0.1326	7.00	0.0695	0.081	0.132	0.05
Trunk	0.6804	36.02	0.4935	0.481	0.322	0.15
Arms	0.2536	13.41	0.0686	0.154	0.095	0.05
Hands	0.0946	5.00	0.1845	0.031	0.121	0.35
Legs	0.5966	31.72	0.1505	0.218	0.230	0.05
Feet	0.1299	6.85	0.0334	0.035	0.10	0.35
Total	1.8877	100.00	1.0000	1.000	1.000	1.00

The total warm receptor output from the skin WARMS can be obtained by summing SKINR (I)* WARM (4* I) for the skin compartments of all six segments (I). The total cold receptor output from the skin can be integrated from a similar summation.

It depends on the concept whether the signals from skin warm receptors are integrated without being offset by simultaneous cold receptor output from other skin areas. Available data is not adequate to clearly determine where integration of cold receptor signals and warm receptor signals takes place, so that the regulator in the controlling system must have either form available. Conceptual regulators which rely on linear addition of thermal signals from different sets of receptors (10, 20) use the ERROR (N) value in the controller equations, whereas conceptual models which use non-linear thermal signals either in a linear (10) or a non-linear expression (1) should use the WARM (N) or COLD (N) values in their controller equations. It will be clear that the weighted skin signal can be recovered in its linear form by subtraction of COLDS from WARMS.

In the suggested controller equations which follow, we have assumed that the central receptors are located in the brain, so that WARM (1), COLD (1) or ERROR (1) constitutes the thermal signal from the interior. There are reasons to believe that central receptors occur elsewhere (25, 28) but not enough is known to take them separately into account, and central temperatures will not normally be found to move far apart, so that lumping central receptors into the brain compartment will only result in a second order error for most circumstances.

In general, the controller equations produce signals which drive the effector part of the regulator. These drives are not necessarily identical to effector action since they may be modified at the effector site by mechanisms responding to local conditions. The controller equations all have a term consisting of the product of a control coefficient and a central temperature signal, a term consisting of the product of a control coefficient and an integrated skin temperature signal and a third term consisting of the product of a control coefficient, a central temperature signal, and a skin temperature signal. Controller equations are then as follows:

SWEAT = CSW* ERROR (1) + SSW* (WARMS-COLDS) + PSW* WARM (1)* WARMS

DILAT = CDIL* ERROR (1) + SDIL* (WARMS - COLDS) + PDIL* WARM (1)* WARMS

CHILL = -CCHIL* ERROR (1) + SCHIL* (COLDS-WARMS) + PCHIL* COLD (1)* COLDS

STRIC = -CCON* ERROR (1) + SCON (COLDS - WARMS)+ PCON* COLD (1)* COLDS

Since these expressions can become negative under certain circumstances, it is necessary to make sure that any negative values of SWEAT, DILAT, CHILL or STRIC are set to zero.

The third part of the controller distributes the effector commands to the appropriate compartment and, if required and appropriate, modifies them according to local conditions.

In order to facilitate the description of this distribution, the following convention will be used: for segment I, the core layer will be indexed as N (equal to 4* I-3), which makes the concentric muscle layer be indexed as (N + 1); the subcutaneous fat layer and the skin layer for segment I then are indicated by the subscripts (N + 2) and (N + 3) respectively. The metabolic rates for all compartments then become as follows:

Q (N) = QB (N)

This expression states that the basal metabolic rate assigned to the cores of the various segments is not thought to vary under the relatively short term conditions for which the model will be used.

$$Q (N + 1) = QB (N + 1) + WORKM (I)^{*} (WORKI) + CHILM (I)^{*} CHILL$$

The metabolic heat production in the muscle compartment is the sum of the basal rate of heat production QB (N + 1), and the sum of the heat production rates assigned due to muscular work done and any shivering thermogenesis. WORKI is the total heat production as one would determine from the oxygen uptake minus the basal metabolic rate and the caloric equivalent of the external work performed. WORKM (I) and CHILM (I) are estimates of the distribution of extra heat production over the various muscle compartments. Th estimates used are given in Table 12.

Table 12

Estimates of Distribution of Heat Production in Muscle Compartments

	% of Total Muscle Mass	WORKM (I)	CHILM (I)
Head	2.323	---	0.02
Trunk	54.790	0.30	0.85
Arms	10.525	0.08	0.05
Hands	0.233	0.01	0.00
Legs	31.897	0.60	0.07
Feet	0.233	0.01	0.00

In the absence of data, the heat from shivering was distributed according to the mass in the various muscle compartments, whereas the values for WORKM (I) are based on estimates for bicycle exercise. Values for WORKM (I) should be reviewed for other types of exercise.

For the subcutaneous fat and the skin compartments, it is assumed that the basal heat production does not change in the conditions to be evaluated by the model, so that:

$$Q\ (N + 2) = QB\ (N + 2)$$

$$Q\ (N + 3) = QB\ (N + 3)$$

The convective heat transfer by blood flow plays a very important role in the thermal responses to internal and external stresses. Certain simplifications are implicit in the expressions which follow. Some of these simplifications are due to a scarcity of applicable data, some of them are justified by the fact that although inaccuracies in mass flow are introduced by the simplifications, these inaccuracies have only a very small effect on heat transfer. For example, it is assumed that blood flow to the core compartment remains at the basal value:

$$BF\ (N) = BFB\ (N)$$

This ignores the fact that blood flow to the trunk core in fact can be reduced during exercise stress (16, 31, 32), but, in fact, the blood flow to these compartments is considerably in excess of that required to supply oxygen to these compartments, so that only small thermal gradients can ever exist between the head core, trunk core and the central blood. Small reductions in core blood flow will then result in slight increases in these small gradients, and convective heat transfer is not materially affected. The muscle compartments, on the other hand, can have widely varying metabolic rates, and substantial variations in blood flow. Regional blood flow measurements over working quadriceps muscle (34) and measurements of arteriovenous oxygen differences across the working quadriceps muscle (35) can be added to measurements of local muscle temperature (36) during exercise to arrive at an insight of muscle blood flow during exercise. Under conditions where heat loss in exercise is mostly from evaporation of sweat, the temperature of the working muscle is about 1.0 °C above that of the arterial blood supplying oxygen (35). If venous blood leaves at muscle temperature, then every liter of blood carries off 0.95 Kcal. Each liter of blood contains about 200 ml O_2 which, if completely scavenged, could produce about 1.0 Kcal of heat. It is thus reasonable to assume that at least 1 l of blood is required to produce 1 Kcal of heat. As a result, the following equation describes the blood flow to the muscle compartments.

$$BF\ (N + 1) = BFB\ (N + 1) + Q\ (N + 1) - QB\ (N + 1)$$

Blood flow to the subcutaneous fat is not very high in basal value, and it is assumed that it is not effectively changed as a result of thermoregulatory adjustments:

$$BF\ (N + 2) = BFB\ (N + 2)$$

Skin blood flow is highly dependent on the thermoregulatory controller. The basal blood flow at thermal neutrality can be reduced to very low values through vasoconstriction, and increased substantially through vasodilatation; in addition, there is an effect of the local temperature which has a substantial modifying influence on resistance of cutaneous veins, as demonstrated by Webb-Peploe and Shepherd (36). These investigators showed that the local temperature of the saphenous vein had a very strong effect on the response of the vein to a given level of constricting stimulation. The peripheral resistance caused by a given level of sympathetic tone would be reduced by high local temperatures and increased by low local temperatures. In many cases, the resistance would about double for a 10°C drop in local temperature, and for a given central signal. The tentative expression for skin blood flow then becomes:

BF (N) = ((BFB (N) + SKINV (I)* DILAT) / (1. + SKINC (I)* STRIC))* 2.**(ERROR (N)/10.)

In this expression, the weighted DILAT drive is added to the basal blood flow. The weighted constrictive tone operates through a resistance and thus is entered as a divisor. The local skin temperature effect then acts on the total flow drive multiplying it by unity in neutral conditions, by less than unity at skin temperatures below normal and by more than one at skin temperatures above the neutral value.

It could be that the local effect on cutaneous veins described by Webb-Peploe and Shepherd does not affect total skin blood flow very much, but reduces heat loss by shifting venous return to deeper veins. This shift would activate an effective counter-current heat exchange between arteries and veins, which could not be distinguished from a reduction in skin blood flow as far as convective heat exchange is concerned.

Evaporative heat loss occurs from the trunk through respiratory water loss, and through evaporation from the skin. Respiratory water loss is a function of the water vapor pressure in the inspired air (PAIR) and the ventilation volume. The ventilation volume is closely related to the metabolic rate, and ventilatory evaporative heat loss can be approximated over a wide range of metabolic rates by:

E (5) = (74.4 + WORKI)* 0.023* (44.0 - PAIR)

in which 44.0 is the vapor pressure in expired air.

For all other core compartments

$$E\ (N) = EB\ (N)$$

and since muscle and subcutaneous fat compartments have no evaporative heat loss:

$$E\ (N + 1) = EB\ (N + 1)$$

$$E\ (N + 2) = EB\ (N + 2)$$

The different skin compartments receive a sweating drive from the central controller. The local response in a given compartment depends on the skin area and on the number of sweat glands present, expressed by SKINS (I). In addition, the local skin temperature modifies the response to a given sweat command as described by Bullard and associates (24).

On repeating these observations in our laboratory, we confirmed the local temperature effect, but found it to have a somewhat lower Q_{10} as shown in Figure 2. As a result, the Q_{10} of the local temperature effect which Bullard, et al. report as about 8 is used here at a value of 2. The evaporative heat loss of the skin of each segment then becomes:

E (N + 3) = (EB (N + 3) + SKINS (I)* SWEAT)* 2.** ((T (N + 3) - TSET (N + 3))/BULL)

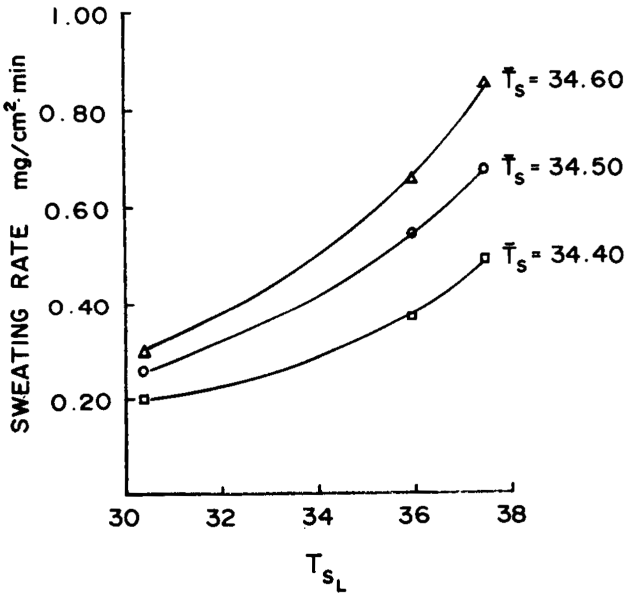

Figure 2. Dependence of local sweat rate on the skin of the thigh, on average skin temperature, and local skin temperature. Internal temperatures were constant during these measurements.

Annotated Listing of FORTRAN Statements Implementing the Model

A flow sheet of the program for simulation of body temperature regulation in man is given in Figure 3, and the listing will follow by sections as identified in the flow diagram.

```
      DIMENSION T(25), TSET (25), RATE (25), C(25), QB(24), EB(24), BFB (24)
      DIMENSION TC(24), S(6), SKINR(6), SKINS (6), SKINV (6), SKINC (6), WORKM (6)
      DIMENSION CHILM (6), HR (6), HC (6), P (10), F (25), H (6), WARM (25), COLD (25)
      DIMENSION HF (25), PSKIN (6)
      DIMENSION ERROR ( 25), Q (24), E (24), BF (24), EMAX (6), BC (24), TD (24)
C
C     READ CONSTANTS FOR THE CONTROLLED SYSTEM
C
  100 FORMAT (14F5.2)
  101 CONTINUE
      READ (2, 100)   C
      READ (2, 100)   QB
      READ (2, 100)   EB
      READ (2, 100)   BFB
      READ (2, 100)   TC
      READ (2, 100)   S
      READ (2, 100)   HR
      READ (2, 100)   HC
      READ (2, 100)   P
      SA = 0.0
      DO 110 K = 1, 6
  110 SA = SA + S (K)
```

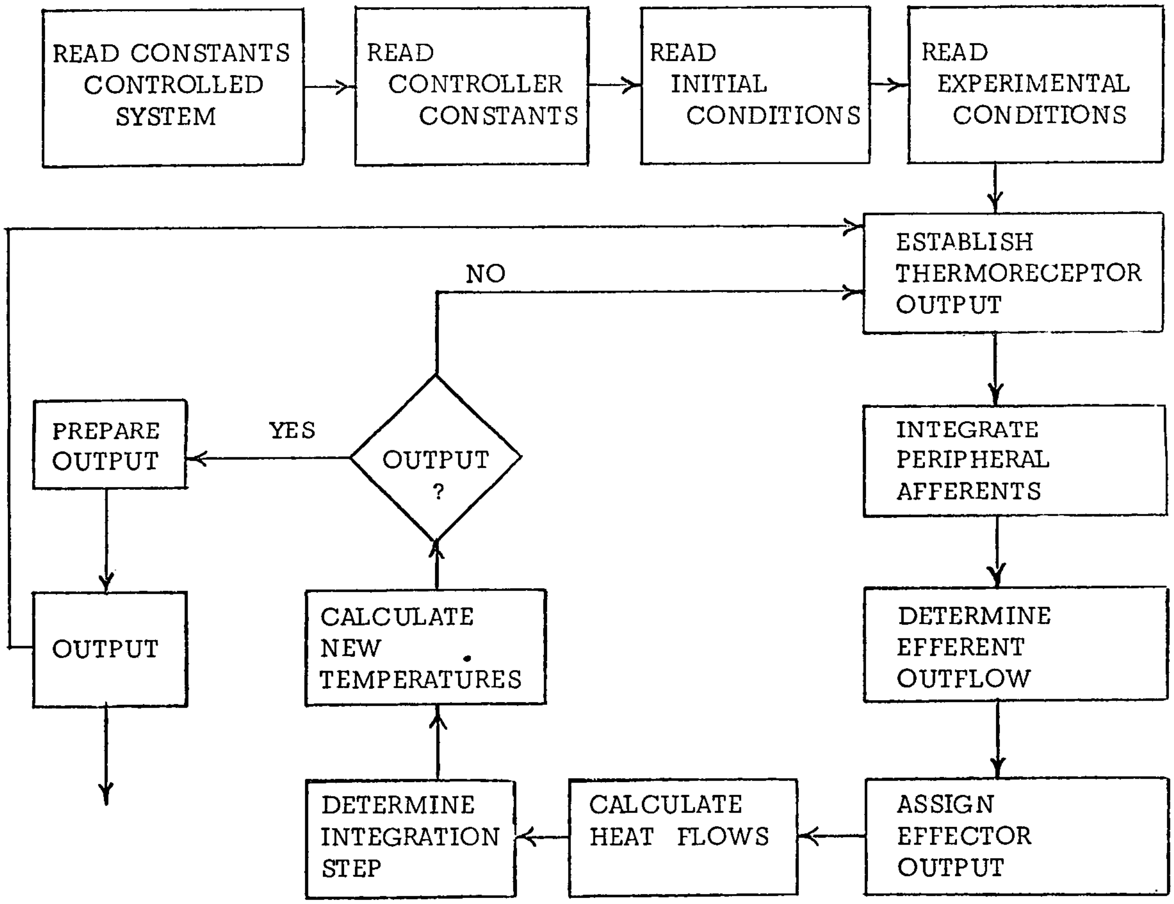

Fig. 3. Flow diagram for simulation of thermoregulation in man

The first section reads in the constants which define the controlled system as defined in the tables before. The values for P are taken from the steam table and consist of the saturated water vapor pressures at 5°C intervals from 5°C to 50°C. Statement 110 calculates the total surface area SA in m^2 for use in the output preparation phase.

The second phase reads in the controller constants beginning with the set point temperatures. As set point temperatures, the values of steady state equilibrium temperatures are used which are reached under the following conditions: air temperature 29.45°C, air velocity 0.1 m/sec, relative humidity 0.3, no work, and all controller coefficients set to 0.0, with the exception of BULL which is set to 10.0.

```
C
C    READ CONSTANTS FOR THE CONTROLLER
C
            READ (2,100)    TSET
            READ (2,100)    RATE
            READ (2,100)    SKINR
            READ (2,100)    SKINS
            READ (2,100)    SKINV
            READ (2,100)    SKINC
            READ (2,100)    WORKM
            READ (2,100)    CHILM
            READ (2,100)CSW,SSW,PSW,CDIL,SDIL,PDIL,CCON,SCON,PCON,
                                                  CCHIL,SCHIL
           XPCHIL, BULL
```

The values for SKINR, SKINS, SKINV, SKINC, WORKM and CHILM have been defined before in preceding Tables 11 and 12.

```
C
C    READ INITIAL CONDITIONS
C
         READ (2,100)  T
         TIME  =  0.0
         ITIME  =  0
         JTIME  =  0
         DO 102 N  =  1, 25
         F (N)  =  0.0
  102    CONTINUE
```

The initial conditions for the next phase consist of the initial values for the temperatures in all compartments. These values are the same as those for TSET and were obtained as described there. The values are given in Table 13.

```
C
C    READ EXPERIMENTAL CONDITIONS
C
         READ (2,299) TAIR, V, RH, WORK, INT
  299    FORMAT (4F5.0, I2)
         IF (WORK - 74.4)     104, 104, 105
  104    WORKI  =  0.0
         GO TO 106
  105    WORKI  =  (WORK - 74.4) * 0.78
  106    CONTINUE
         DO 202 I  =  1, 6
         H(I)  =  (HR(I) + HC (I) * (V/O.1) **0.5) * S (I)
  202    CONTINUE
         I  =  TAIR/5
         PAIR = RH*(P(I) + (P (I + 1) - P (I) )*(TAIR - 5 * I)/5.0)
```

Table 13

Set Point Values and Initial Condition Temperatures

Segment	Compartment	N	Temperature °C
Head	Core	1	36.96
	Muscle	2	35.07
	Fat	3	34.81
	Skin	4	34.58
Trunk	Core	5	36.89
	Muscle	6	36.28
	Fat	7	34.53
	Skin	8	33.62
Arms	Core	9	35.53
	Muscle	10	34.12
	Fat	11	33.59
	Skin	12	33.25
Hands	Core	13	35.41
	Muscle	14	35.38
	Fat	15	35.30
	Skin	16	35.22
Legs	Core	17	35.81
	Muscle	18	35.30
	Fat	19	35.31
	Skin	20	34.10
Feet	Core	21	35.14
	Muscle	22	35.03
	Fat	23	35.11
	Skin	24	35.04
Central Blood		25	36.71

The next phase reads in the experimental conditions, air temperature, air velocity in m. sec^{-1}, the relative humidity as a fraction rather than a percentage, the work rate in total heat production in $Kcal.h^{-1}$ as normally computed from oxygen uptake, and the interval in minutes between desired outputs. Next, WORKI is computed by subtracting the basal metabolic rate, and by subtracting the external work, so that WORKI represents the total extra heat production in the working muscle. Subsequently, H(I) is calculated in $Kcal.h^{-1} . °C^{-1}$ for each segment. The last two statements look up the partial pressure of water vapor in the environment by interpolation from the steam table.

```
C
C   ESTABLISH THERMORECEPTOR OUTPUT
C
          301   CONTINUE
                DO 302 N = 1, 25
                WARM (N)  =  0.0
                COLD (N)  =  0.0
                IF (F(N) ) 310, 311, 311
          311   F (N)  =  0.0
          310   CONTINUE
                ERROR (N) = T (N) - TSET (N) + RATE (N) * F (N)
                IF (ERROR (N) )  303, 302, 304
          303   COLD (N)  =  ERROR (N)
                GO TO 302
          304   WARM (N)  =  ERROR (N)
          302   CONTINUE
```

In the next phase, the actual instantaneous temperatures in all compartments are compared with the "set point" temperatures, taking into account the rate of change in those cases where this is appropriate. The direction of rate of change is first determined, and positive rates of change are set to zero. This was done because we have not been able to demonstrate specific effects of a positive rate of change, although a direct effect of negative rate of change of skin temperature on sweating has been demonstrated. Such effects had been implied earlier (37) and were studied quantitatively in our laboratory by Nadel, Bullard and Stolwijk (38). In these experiments it was shown that local sweating rate as measured by a sweat capsule and resistance hygrometry was linearly dependent on average skin temperature, as long as local skin temperature and internal temperatures were held constant. Radiant energy was used to bring about rapid changes in average skin temperature. Figure 4 shows such linear dependence on average skin temperature at various local skin temperature, in a steady state condition. When rapid changes were brought about, it was found that during skin warming the instantaneous mean skin temperature was a good predictor of instantaneous local sweat rate, but during cooling the sweat rate at any instant was lower than that predicted by instantaneous mean skin temperature. It was found that this deviation was proportional to the negative rate of change in average skin temperature as shown in Figure 5.

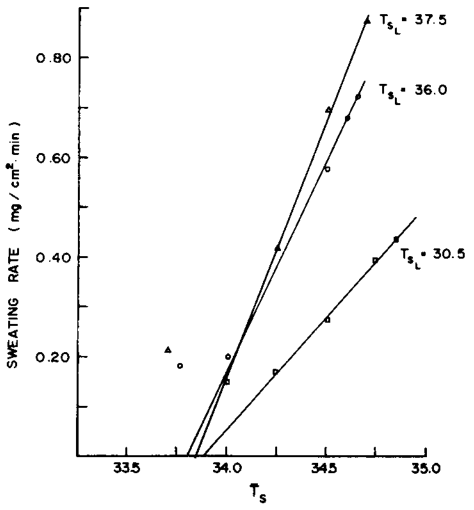

Figure 4. Linearity of local sweating response with average skin temperature, at constant internal temperature.

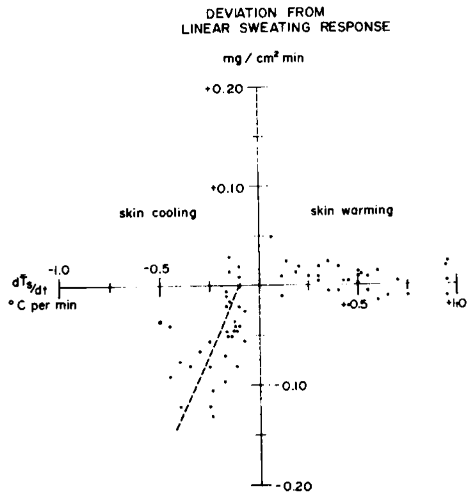

Figure 5. Deviation from sweating response linear with average skin temperature, as a function of rate of fall of mean skin temperature.

This phase results in lists of temperature deviations from normal, in linear terms (ERROR (N)) and in non-linear terms WARM (N) and COLD (N) which are zero for values below and above the set point respectively.

```
C
C   INTEGRATE PERIPHERAL AFFERENTS
C
          WARMS = 0.0
          COLDS = 0.0
          DO 305 I = 1, 6
          K = 4*I
          WARMS = WARMS + WARM (K) * SKINR (I)
          COLDS = COLDS + COLD (K) * SKINR (I)
      305 CONTINUE
```

Since only the skin afferents are used in the present model, these signals are the only ones to be weighted for integration. Weighting is done according to the receptor density estimates SKINR (I). The use of WARM (K) and COLD (K) does not necessarily cause the loss of linear information. A linear form of the weighted value of the skin error signal can be recovered by the use of WARMS - COLDS.

```
C
C   DETERMINE EFFERENT OUTFLOW
C
      SWEAT = CSW*ERROR(1) +SSW * (WARMS-COLDS) + PSW * WARM (1) * WARMS
      DILAT = CDIL * ERROR (1) + SDIL * (WARMS - COLDS) + PDIL * WARM (1) * WARMS
      STRIC = -CCON * ERROR (1) -SCON* (WARMS - COLDS) + PCON * COLD (1) * COLDS
      CHILL = -CCHIL * ERROR (1) -SCHIL * (WARMS-COLDS) + PCHIL * COLD (1) * COLDS
      IF (SWEAT) 309, 312, 312
  309 SWEAT = 0.0
  312 IF (DILAT) 313, 314, 314
```

```
313 DILAT = 0.0
314 IF (STRIC) 315, 316, 316
315 STRIC = 0.0
316 IF (CHILL) 317, 318, 318
317 CHILL = 0.0
318 CONTINUE
```

The next section calculates the control commands going to the periphery. Since the ERROR (N) terms can become negative as well as positive, each of the commands is protected against becoming negative.

```
C
C   ASSIGN EFFECTOR OUTPUT TO THE COMPARTMENTS
C
    400     CONTINUE
            DO 401 I = 1, 6
            N = 4 * I - 3
            Q (N) = QB (N)
            BF (N) = BFB (N)
            E (N) = EB (N)
            Q (N + 1) = QB (N + 1) + WORKM (I) * WORKI + CHILM (I) * CHILL
            E (N + 1) = 0.0
            BF (N + 1) = BFB (N + 1) + Q (N + 1) - QB (N + 1)
            Q (N + 2) = QB (N + 2)
            E (N + 2) = 0.0
            BF (N + 2) = BFB (N + 2)
            Q (N + 3) = QB (N + 3)
            E(N + 3) = (EB (N+3) + SKINS (I) * SWEAT) * 2.0 ** (ERROR (N+3) / BULL)
            BF (N+3) = ( (BFB (N+3) + SKINV (I) * DILAT)/(1.0+SKINC (I)* STRIC) )* 2.0**
           X(ERROR (N + 3) / 10.0)
```

```
        K = T (N + 3)/5
        PSKIN (I) = P (K) + (P (K + 1) -P(K)) * (T (N + 3) -5*K)/5.0
        EMAX (I) = (PSKIN (I) -PAIR) *2.2 * (H (I) -HR (I) * S (I) )
        IF (E (N + 3) -EMAX (I))  403, 403, 402
402     E (N + 3) = EMAX (I)
403     CONTINUE
401     CONTINUE
        E (5) = (74.4 + WORKI) * 0.0023 * (44.0 -PAIR)
```

This phase distributes the control commands to the various segments and within the segments to compartments in the form of the calculated effect of heat flow in Kcal . h^{-1} for Q (N) and E (N), and of conductance in Kcal . h^{-1} . $°C^{-1}$ for BF (N). The core compartments (N) and the fat compartments (N + 3) remain at basal values. The muscle compartments receive their assigned portion of the total internal heat production due to work, and of that due to shivering. For each Kcal of heat produced, the muscle requires at least one liter of blood, as seen in BF (N + 1).

Skin metabolic rate remains at basal values, but skin blood flow and evaporative heat loss are determined by command signals, as modified by the local temperature.

The water vapor pressure at the skin surface temperature is read and interpolated from the steam table and the maximum evaporative heat loss from a completely wet skin EMAX (I) is computed, based on existing conditions. If the computed evaporation from the skin E (N + 3) exceeds the maximum possible EMAX (I), then the former is set equal to EMAX (I). The last statement calculates the evaporative heat loss from the respiratory tract with the aid of total metabolic rate and the water vapor pressure in the environment.

```
C
C   CALCULATE HEAT FLOWS
C
        DO 500 K = 1, 24
        BC (K) = BF (K) * (T (K) -T (25) )
        TD (K) = TC (K) * (T (K) -T (K + 1) )
  500   CONTINUE
        DO 501 I = 1, 6
        K  =  4 * I-3
        HF (K) = Q (K) -E (K) -BC (K) -TD (K)
        HF (K + 1) = Q (K + 1) -BC (K + 1) + TD (K) -TD (K + 1)
        HF (K + 2) = Q (K + 2) -BC (K + 2) + TD (K + 1) -TD (K + 2)
        HF (K + 3) = Q (K + 3) -BC (K + 3) -E (K + 3) + TD (K + 2) -H(I) * (T(K+3)-TAIR)
  501   CONTINUE
        HF (25) = 0.
        DO 502 K = 1, 24
        HF (25) = HF (25) + BC (K)
  502 CONTINUE
```

The next section computes the net heat flow rates into or out of each of the compartments. Initially BC (K), the convective heat flow rate, and TD (K), the conductive heat flow rate for each compartment to the next compartment are calculated. After this, all the heat flow rate components are added up for each compartment. The only exception is the central blood compartment which receives the sum of all convective heat flows.

```
C
C   DETERMINE OPTIMUM INTEGRATION STEP
C
            DT = 0.016666666667
            DO  600  K = 1, 25
            F (K)  =  HF (K)/C (K)
            U  =  ABS (F (K))
            IF (U * DT -0.1)    600, 600, 601
    601     DT  =  0.1/U
    600     CONTINUE
```

The optimum integration time step is determined in the next phase. Initially the time increment for numerical integration is set to 0.01667 hours or 1 minute this being considered the shortest plausible print-out interval. Based on this increment, the temperature steps in each compartment are calculated and if any exceed 0.1°C then the time increment DT is reduced so that the maximum temperature change in any compartment in each iteration is kept to 0.1°C or less.

```
C
C   CALCULATE NEW TEMPERATURES
C
            DO  700  K = 1, 25
            T (K) = T (K) + F (K) * DT
    700     CONTINUE
            TIME  =  TIME + DT
            LTIME = 60. * TIME
            IF (LTIME -INT -ITIME)   301, 701, 701
    701     CONTINUE
```

Based on the time increment thus arrived at, the next section calculates the new temperatures and increments the clock with the value of the integration increment DT. This followed by a test to see whether output is desired. If such output is not desired, the program returns to the phase where thermoreceptor output is re-computed. If output is desired, the program proceeds to the next phase.

```
C
C     PREPARE FOR OUTPUT
C
            EWET = 0.0
            DO 450 I = 1, 6
            EWET = EWET + (E(4 * I)/EMAX (I) ) * (S (I)/SA)
      450   CONTINUE
            PWET = 100. * EWET
            ITIME = ITIME + INT
            CO = 0.0
            HP = 0.0
            EV = 0.0
            TS = 0.0
            TB = 0.0
            HFLOW = 0.0
            SBF = 0.0
            DO 800 N = 1, 24
            CO = CO + BF (N)/60.0
            HP = HP + Q (N)
            EV = EV + E (N)
      800   CONTINUE
            DO 802 I = 1, 6
            SBF = SBF + BF (4 * I)/60.0
            TS = TS + T (4 * I) * C (4 * I)/3.35
```

```
802     CONTINUE
        DO 801  N = 1, 25
        TB = TB + T (N) * C (N)/59.17
        HFLOW = HFLOW + HF (N)
801     CONTINUE
        EV = EV/SA
        HP = HP/SA
        HFLOW = HFLOW/SA
        COND = (HP -E(5)/SA -HFLOW)/(T (25) -TS)
```

In this phase, the value of variables which refer to compartments or segments are combined to yield values in the dimensions usually used for reporting thermo-physiological experiments. The first few statements calculate the fractional wetted area of the skin according to Gagge (13) from the area-weighted ratios of the actual evaporation rate and the maximum possible evaporation rate. The output time clock is incremented with one print-out interval time. The cardiac output, heat production and evaporative heat loss are obtained by summing of blood flow, metabolic heat production rate and evaporative heat loss over all compartments. Skin blood flow, SBF, and mean skin temperature,TS, are calculated by summing of segmental skin blood flows and skin temperatures. Similarly, mean body temperature is obtained by averaging of all compartmental temperatures weighted with their thermal capacitance. Net rate of heat storage for the whole body is obtained by summing all net heat flow over all compartments. EV, HP and heat flow are reduced to Kcal . m^{-2} . h^{-1} by dividing them by the total body surface area SA. The core-to-skin thermal conductance, COND, which is often derived in physiological experiments is derived in the conventional manner.

The next phase contains the output statements which are not a material part of the program and which would normally depend on the purpose for which the simulation is intended.

```
C
C   BEGINNING OF OUTPUT SECTION
C
          CALL DATSW (0, K)
          GO TO (951, 950), K
    951   CONTINUE
          IF (ITIME -INT) 909, 909, 911
    909   PAUSE
    910   WRITE (1, 912)
    912   FORMAT ('TIME  S  M  EV  TB  TS  TH  TO  TR  TM  1  SBF  CO  COND  PWET')
          NN  =  0
    911   IF (NN-42) 913, 913, 914
    913   WRITE (1, 915) ITIME, HFLOW, HP, EV, TB, TS, T(1), T(25), T(5), T(18), SBF,
          CO, 1  COND, PWET
    915   FORMAT (13, 3F7.1, 8F6.2, 2F6.1)
          NN  =  NN + 1
          GO TO 1100
    914   WRITE (1, 916)
    916   FORMAT (22(/) )
          GO TO 910
    950   CONTINUE
   1100   JTIME  =  JTIME + INT
          CALL DATSW (1, K)
          GO TO (917, 1102), K
```

```
917  CONTINUE
     ITA = TAIR * 10.
     ISKSW = 1.16 * (EV-9.5-0.08 * WORK/SA)
     IHP = HP
     ITS = TS * 100.
     ITR = T (5) * 100.
     ITO = T (25) * 100.
     ITM = T (18) * 100.
     IEV = EV
     ICOND = COND * 1.16
     IRM = HP * 1.16
     ITB = TB * 100.
     WRITE (2, 9901) ITIME, ITA, IHP, ITS, ITR, ITO, ITM, IEV, ISKSW, ICOND,
    IRM, XITB, SBF, CO
9901 FORMAT (3I3, 4I4, 3X, I3, 3X, 3I3, 4X, I4, F4.2, F5.2)
1102 IF (JTIME-30) 301, 1101, 1101
1101 JTIME = 0
     PAUSE
     IF (ITIME-210) 102, 101, 101
9990 CALL LEAVE
901  CALL EXIT
     END
```

Control Coefficients

As will be evident from simulations shown later, it is not yet possible to account for all experimental results with a single set of control coefficients. This section is concerned with the description of current controller concepts and values of control coefficients and the experimental justification and validation. It will be seen that there is a tendency to obtain values from a variety of steady state responses with backgrounds as diverse as possible, and to attempt to validate them under dynamic conditions. The dynamic conditions do not only test the validity of concept and quantitative character of the controller, but they also challenge the validity of the controlled system as described here. The relatively small number of nodes in the finite difference method used here does impose a limit on the time resolution which can usefully be obtained, especially in conditions where large gradients exist, or where vasoconstriction reduces convective heat transfer.

Control of Sweating

We have available in the results obtained in this laboratory in resting experiments and exercise experiments the basic information to describe the control of sweating. Figure 6 shows a composite plot of more or less steady state rates of sweating as dependent on internal temperature and skin temperature, taken from (10, 11, 30). The broken line demarcates the area outside which, for physical or physiological reasons, it would be hard or impossible to produce a steady state.

It is clear that the different lines of equal mean skin temperatures have different slopes as well as intercepts. From Figure 6 and Figure 4, we can then draw the following conclusions:

1. At constant skin temperature, sweating is proportional to internal temperature (Figure 6).

2. At constant internal temperature, sweating is proportional to mean skin temperature (Figure 4).

3. At a given combination of internal temperature and mean skin temperature, the local sweating is dependent on local skin temperature with a Q_{10} of about 2 (Figure 4).

It is clear then that Figure 6 has included in it this local effect. By making the arbitrary assumption that the mean skin temperature at thermal neutrality is the "normal" one for referencing the peripheral Q_{10} effect, we can eliminate the local effect from Figure 6 and this produces Figure 7 which then represents the output from the central controller. The expression of the controller output in Figure 7 then becomes:

SWEAT = 320. * ERROR (I) + 29. * (WARMS - COLDS) so that

CSW = 320.0   SSW = 29.0 and PSW = 0.0 become the controller coefficients for the central controllers. From Figure 6, it can be derived that the local skin temperature effect has a Q_{10} of 2 so that the local coefficient BULL = 10.0, and the local multiplier becomes: 2.0 ** (ERROR (N + 3) / 10.0).

This concept of the control of sweating thus contains the additive as well as multiplicative aspects of integration of central and peripheral signals, and, moreover, does not require for steady state conditions a non-thermal factor which has been postulated.

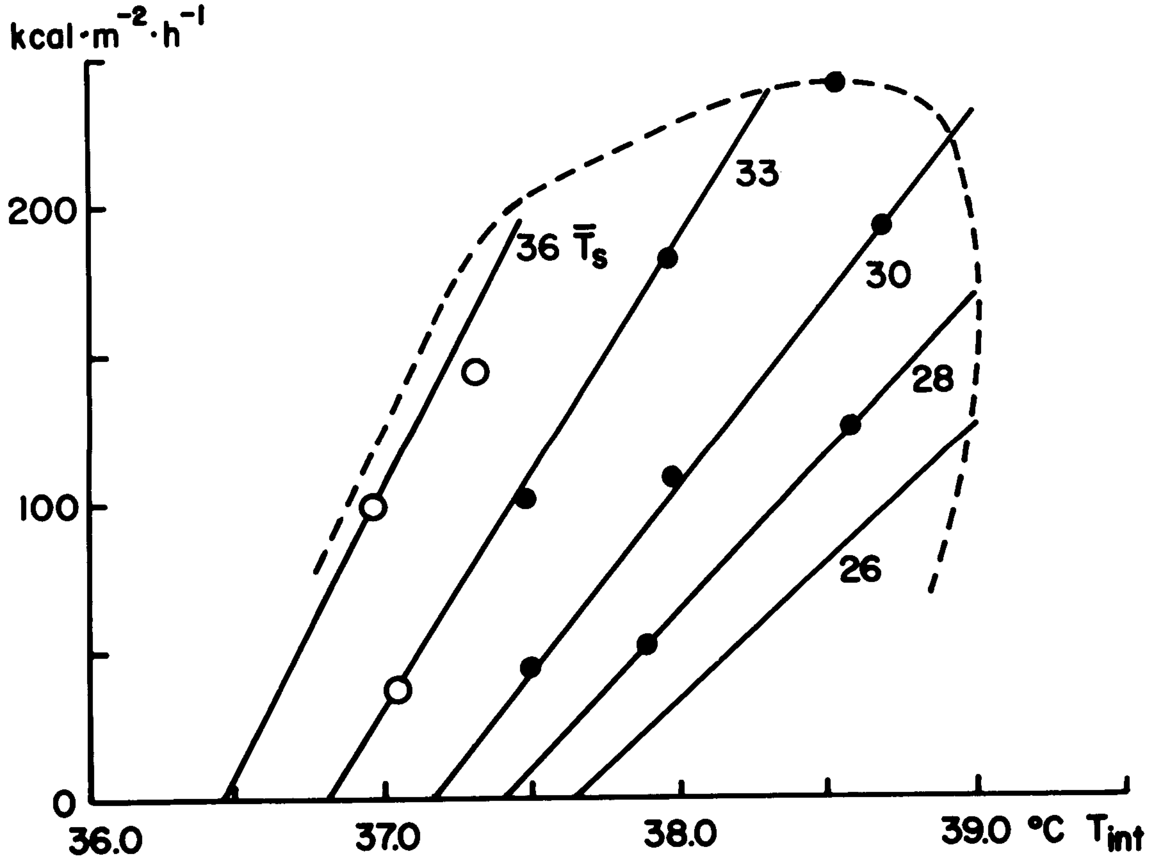

Figure 6. Composite plot of more or less steady state rates of sweating as dependent on internal temperatures.

Control of Vasodilatation

Measurements of peripheral vasodilatation is not directly possible as is the case with sweating. The most widely used measurement is a derived one usually indicated by the symbol K which is the effective thermal conductance from core to skin surface, expressed in Kcal . m^{-2} . h^{-1} . $°C^{-1}$; K is calculated from:

$$COND = (HP - E(5) - HFLOW)/((T(5) - TS)/SA)$$

It is implicit in the definition that the thermal conductance can only be calculated during conditions where no gradients are changing; i.e., in quasi-steady states. Such values have more inherent fluctuation than direct measurements so that the plot assembling such values from a number of experimental conditions from (10, 11, 30) is not as orderly as that for sweating. The plot is given in Figure 8. The similarity of this plot to that of Figure 6 is probably not altogether coincidental, in view of the similarity between the Bullard, et al. (24) findings for the action of peripheral temperature on sweat gland response, and the findings of Webb - Peploe and Shepherd (36) on the action of peripheral temperature directly on the responsiveness of cutaneous veins to sympathetic tone.

If we may make the not yet completely proven assumption that the similarity is more than suggestive, it is useful to derive control equations for the central vasodilatory drive in a manner similar to that in the case of sweating. Figure 10 then shows the value of K for different values of central temperature and mean skin temperature, with the local peripheral effect removed, again normalizing at the skin temperature at thermal neutrality. It is then found that the slope of the lines is 62 l . m^{-2} . h^{-1} . $°C^{-1}$ if we equate an increase of 1 Kcal . m^{-2} . h^{-1} . $°C^{-1}$ in the conductance with at least 1 l . h^{-1} . m^{-2} increase in skin blood flow. It then also follows that 1 °C change in mean skin temperature at constant internal temperature results in about 4 $l \cdot m^{-2} \cdot h^{-1}$ change in skin blood flow. The controller command then becomes:

DILAT = 117. * ERROR (I) + 7.5 * (WARMS - COLDS)

so that CDIL = 117.0, SDIL = 7.5 and PDIL = 0.0

It also becomes clear that the local effect causes a doubling or halving of local blood flow for a 6°C change in local temperature, so that the local multiplier becomes:

2.0** (ERROR (N + 3) / 6.

The value for the central control coefficient CDIL of 117.0 is very close to one proposed in earlier reports and also compares with a value of about 90 proposed by Benzinger, et al. (39).

Control of Shivering

Shivering, although easily measured, is among the elusive physiological responses since steady states are difficult to obtain. However, a large number of measurements all point to the fact that both skin temperature and internal temperature must be below a certain threshold. Such measurements were made by Benzinger, et al. (39) and by Nadel (40). Probably as a result of differences in methods, these authors find slightly different values for the threshold for the central and mean skin temperatures. These authors, as do many others, report responses which can consistently be predicted by a multiplicative expression. Measurements in this laboratory have failed to give responses which were consistent enough to use for quantitative extrapolation. One very consistent difference was found in that for a given cold exposure women shivered earlier and to a much higher degree

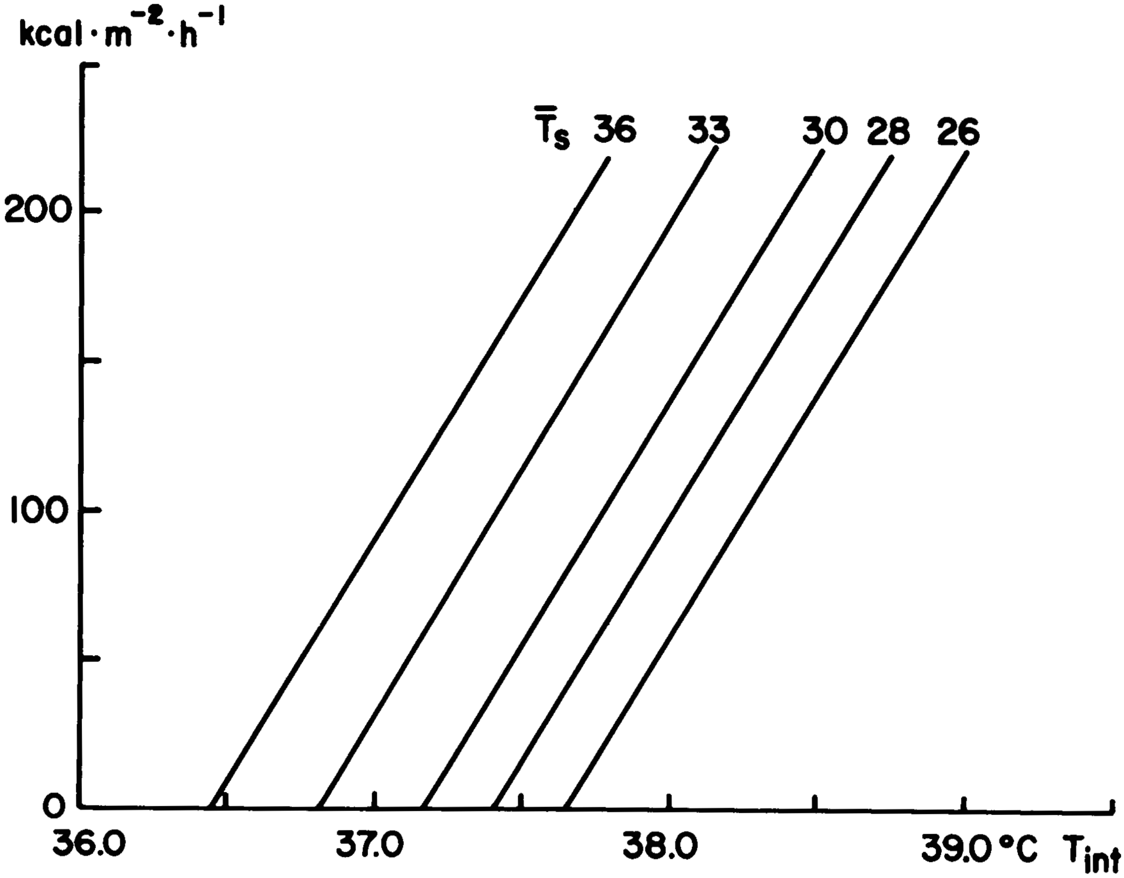

Figure 7. Output from the central controller.

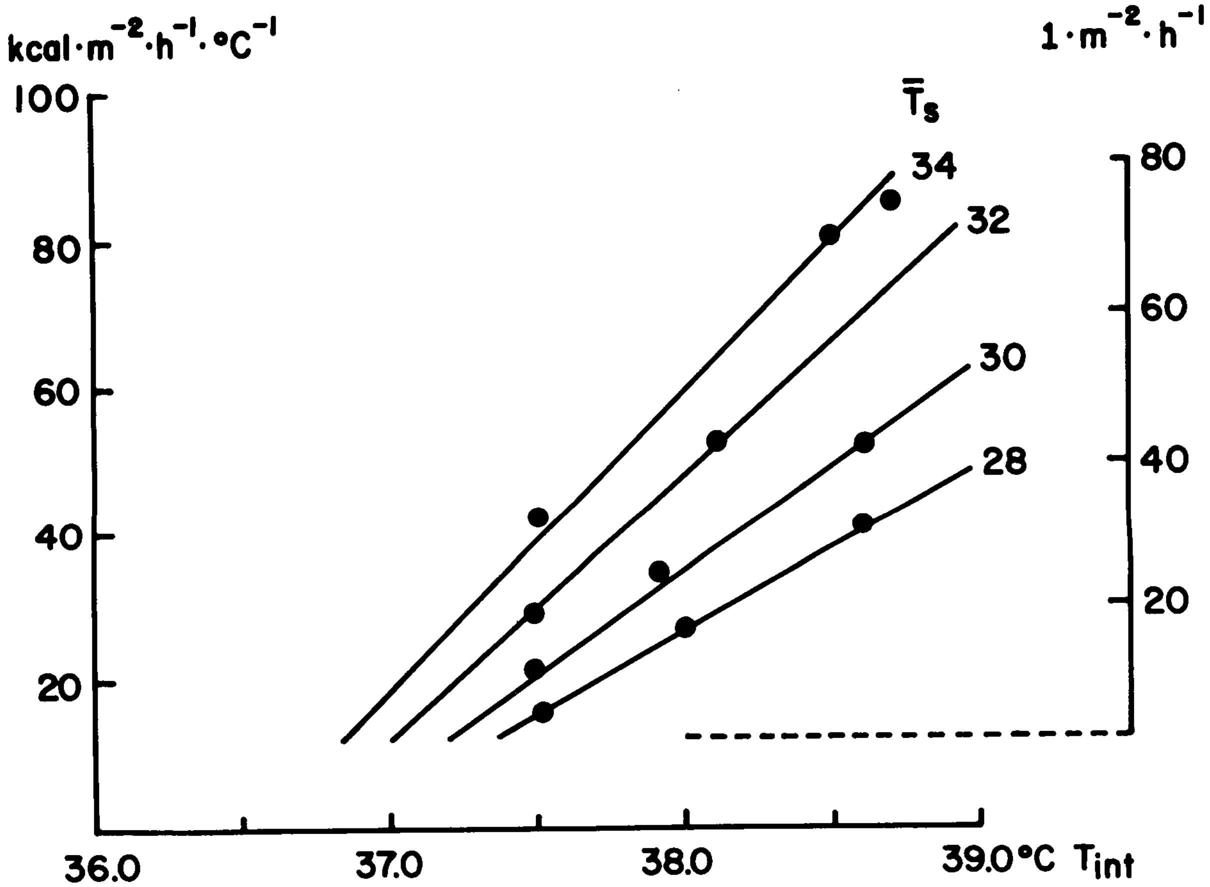

Figure 8. Plot of a number of experimental conditions.

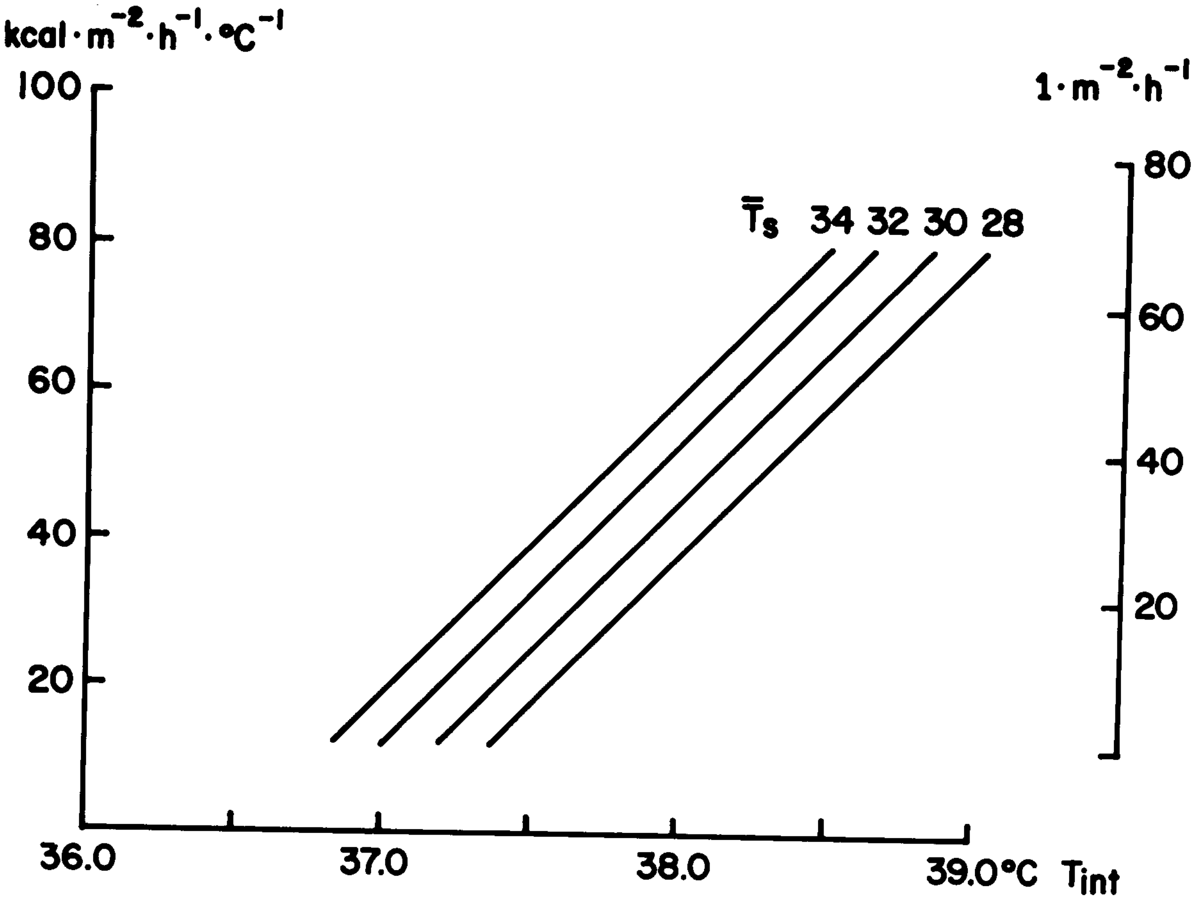

Figure 9. Experimental profile.

than men. Women also showed a more labile vasomotor response in heat and cold and had a consistently lower CSW value than men. The latter difference resulted in women reaching higher internal body temperatures during resting heat exposure. A detailed report on these experiments is in preparation. Benzinger, et al. (39) report results which would suggest that in the expression for shivering control the following value should be used:

$$\text{CHILL} = 21.0 * \text{COLD (I)} * \text{COLDS}$$

which would result in the following control coefficients:

$$\text{CCHIL} = 0.0, \quad \text{SCHIL} = 0.0 \text{ and PCHIL} = 21.0.$$

Nadel's results would indicate a higher value for PCHIL in the range of 40.0, but his measurements were short lasting and should, therefore, be approached with more caution.

Control of Vasoconstriction

The type of vasoconstriction implied here is largely limited to the special peripheral vascular beds in the hands and feet which normally have a high non-nutritive blood flow which is highly sensitive to both internal temperature and mean skin temperature. In addition, there is a high sensitivity to psychogenic disturbances. As the mean skin temperature decreases below normal, or as the central temperature decreases below normal, constrictor tone in hands and feet increase. Since this represents an increase in resistance, the calculated local blood flow is reduced by dividing it by a value STRIC. In the absence of clear data, the following expression is used to define STRIC:

$$\text{STRIC} = -5.0 * (\text{ERROR (I)} + \text{WARMS} - \text{COLDS}).$$

Table 14

TIME	S	M	EV	TB	TS	TH	TO	TR	TM	SBF	CO	COND	PWET
5	2.0	40.2	7.6	35.75	33.89	36.98	36.77	36.93	35.30	0.10	4.68	12.1	2.6
10	1.9	39.9	7.6	35.76	33.85	37.01	36.81	36.97	35.30	0.10	4.67	11.7	2.6
15	1.8	39.5	7.5	35.76	33.82	37.05	36.84	37.01	35.30	0.10	4.66	11.4	2.6
20	1.8	39.4	7.5	35.77	33.80	37.08	36.87	37.04	35.30	0.10	4.65	11.2	2.6
25	1.9	39.4	7.5	35.77	33.79	37.10	36.89	37.06	35.30	0.10	4.65	11.0	2.6
30	1.9	39.4	7.5	35.78	33.78	37.12	36.91	37.08	35.30	0.10	4.65	10.9	2.6
35	82.9	39.4	38.8	36.05	36.10	37.12	36.90	37.08	35.38	0.51	5.06	-56.0	34.9
40	55.2	39.4	63.6	36.24	36.48	37.22	37.01	37.15	35.57	0.78	5.33	-33.1	55.9
45	41.0	39.4	77.4	36.35	36.53	37.31	37.08	37.24	35.77	0.98	5.53	-6.0	67.7
50	31.9	39.4	86.2	36.45	36.57	37.38	37.13	37.30	35.94	1.16	5.71	10.3	73.8
55	26.4	39.4	91.5	36.52	36.59	37.42	37.16	37.34	36.08	1.26	5.82	19.8	77.6
60	23.2	39.4	94.6	36.59	36.61	37.44	37.18	37.36	36.21	1.32	5.88	25.4	79.8
65	21.2	39.4	96.5	36.65	36.63	37.46	37.20	37.38	36.31	1.37	5.92	29.1	81.0
70	19.3	39.4	98.2	36.70	36.66	37.48	37.22	37.40	36.40	1.41	5.97	32.8	82.0
75	17.8	39.4	99.6	36.75	36.68	37.49	37.23	37.42	36.48	1.45	6.00	35.7	82.8
80	16.6	39.4	100.7	36.80	36.69	37.51	37.24	37.43	36.56	1.48	6.04	38.3	83.5
85	15.4	39.4	101.7	36.84	36.71	37.52	37.26	37.45	36.63	1.51	6.07	40.7	84.1
90	14.2	39.4	102.8	36.88	36.73	37.53	37.27	37.46	36.69	1.55	6.10	43.1	84.7
95	13.3	39.4	103.6	36.92	36.74	37.54	37.28	37.47	36.74	1.57	6.13	44.8	85.2
100	12.2	39.4	104.6	36.95	36.75	37.56	37.29	37.48	36.80	1.61	6.16	47.0	85.7
105	11.5	39.4	105.4	36.98	36.76	37.57	37.30	37.49	36.83	1.63	6.18	48.5	86.2
110	10.6	39.4	106.2	37.01	36.77	37.57	37.31	37.50	36.87	1.66	6.21	50.2	86.7
115	10.0	39.4	106.7	37.04	36.78	37.58	37.32	37.51	36.91	1.67	6.23	51.4	87.0
120	9.3	39.4	107.3	37.07	36.79	37.59	37.33	37.52	36.94	1.69	6.25	52.7	87.3
125	8.7	39.4	107.8	37.09	36.79	37.60	37.33	37.53	36.97	1.71	6.26	53.8	87.6
130	8.2	39.4	108.3	37.11	36.80	37.61	37.34	37.53	37.00	1.73	6.28	54.8	87.9
135	7.5	39.4	109.0	37.13	36.81	37.61	37.34	37.54	37.02	1.75	6.30	56.1	88.3
140	7.1	39.4	109.4	37.15	36.81	37.62	37.35	37.55	37.05	1.76	6.31	57.0	88.6
145	6.6	39.4	109.8	37.17	36.82	37.62	37.35	37.55	37.07	1.77	6.33	57.8	88.8
150	6.2	39.4	110.2	37.18	36.82	37.63	37.36	37.56	37.09	1.79	6.34	58.6	89.0
155	-70.1	39.4	70.4	36.92	35.09	37.39	36.99	37.31	37.04	0.92	5.47	55.8	37.6
160	-37.1	39.4	39.0	36.79	34.89	37.23	36.94	37.16	36.93	0.55	5.11	35.9	20.3
165	-26.0	39.4	28.5	36.71	34.80	37.18	36.93	37.12	36.82	0.44	4.99	29.3	14.4
170	-21.0	39.4	24.0	36.64	34.71	37.16	36.93	37.12	36.71	0.38	4.93	25.9	11.9
175	-18.9	39.4	22.5	36.59	34.64	37.17	36.93	37.12	36.63	0.34	4.89	24.0	11.0
180	-17.1	39.4	21.3	36.55	34.56	37.17	36.94	37.12	36.55	0.31	4.86	22.4	10.5
185	-15.8	39.4	20.5	36.50	34.48	37.17	36.94	37.13	36.47	0.29	4.84	21.2	10.0
190	-14.6	39.4	19.6	36.46	34.43	37.17	36.94	37.13	36.41	0.27	4.83	20.2	9.6
195	-13.5	39.4	18.9	36.42	34.38	37.17	36.94	37.13	36.35	0.26	4.81	19.4	9.1
200	-12.5	39.4	18.2	36.39	34.34	37.17	36.94	37.13	36.30	0.25	4.80	18.7	8.8
205	-11.5	39.4	17.5	36.35	34.29	37.17	36.94	37.13	36.24	0.24	4.79	18.0	8.4
210	-10.7	39.4	16.9	36.33	34.27	37.17	36.94	37.13	36.20	0.23	4.79	17.5	8.0

Performance of Model of Thermoregulation in Man at Rest

It is easily recognized that the model will reproduce the steady state thermoregulatory responses with acceptable accuracy since the control coefficients are essentially based on steady state relationships. The best method of validation then is to reproduce a sudden change in conditions with the resultant dynamic thermoregulatory response. In order to do this, two specific experiments were simulated which were also evaluated with an earlier model (1). Young male subjects were quickly transferred between two ambient temperatures; the air and wall temperatures were equal, and the air velocities were minimal (i.e., 0.1 m/sec or less). Average skin temperature, rectal temperature, tympanic membrane temperature, rate of evaporative weight loss and metabolic rate were determined continuously. The experiments have been described in more detail before (10, 11). Figure 10 shows an experiment in which the subject spent 30 minutes at a thermally neutral temperature, followed by 120 minutes at an ambient temperature of 48°C, and an additional 60 minutes of recovery in a 30°C environment. In each case, the broken line represents the response predicted by the model, and the solid line shows the experimental result, in measurements of rectal temperature, mean skin temperature and sweat rate. The metabolic rate, during the whole experiment, stayed in the range of 38 - 42 Kcal . m^{-2} . h^{-1}. The results predicted by the model are given in more detail in Table 14. The headings in Table 14 and other tables following after Table 14 are abbreviations for the following variables: TIME, in minutes; S: rate of heat storage in Kcal . m^{-2} . h^{-1}; M: metabolic heat production in Kcal . m^{-2} . h^{-1}; EV: total evaporative heat loss in Kcal . m^{-2} . h^{-1}; TB: mean weighted body temperature in °C; TS: mean weighted skin temperature in °C; TH: temperature of the head core representing hypothalamic temperature in °C; TO: temperature of the central blood compartment, representing esophageal temperature in °C; TR: trunk core temperature representing rectal temperature in °C; TM: temperature of the muscle compartment in the leg in °C; SBF: total skin blood flow in $1 \cdot min^{-1}$; CO: estimated cardiac output in $1 \cdot min^{-1}$; COND: equivalent thermal conductance from core to skin, $Kcal \cdot m^{-2} \cdot h^{-1} \cdot °C^{-1}$; PWET: percentage of the skin surface as wetted area (13, 14) for the sweat rate and environmental conditions given.

In a different type of experiment, the subjects spent 60 minutes at an environmental temperature of 43°C followed by 120 minutes at 17°C and a final 30 minutes at 43°C. Data and simulation of this experiment are given in Figure 11 and Table 15. In the experiment, the metabolic rate remained at near basal levels and descended continuously from an initial 45 $Kcal \cdot m^{-2} \cdot h^{-1}$ to a final 36 $Kcal \cdot m^{-2} \cdot h^{-1}$. It will be seen from Table 15 that in the simulation some shivering started after about one hour in the cold, and it remained at one basal metabolic rate through much of the remaining hour. In the experiment, there was a continuing negative heat storage of about 37 $Kcal \cdot m^{-2} \cdot h^{-1}$ throughout that same hour. In the experiment, it was calculated that the total net heat loss during the cold exposure amounted to 92 $Kcal \cdot m^{-2}$ or about a 2.6°C drop in mean body temperature. We have also observed that the model response to this regimen of cold exposure is very close to that shown consistently by women subjects.

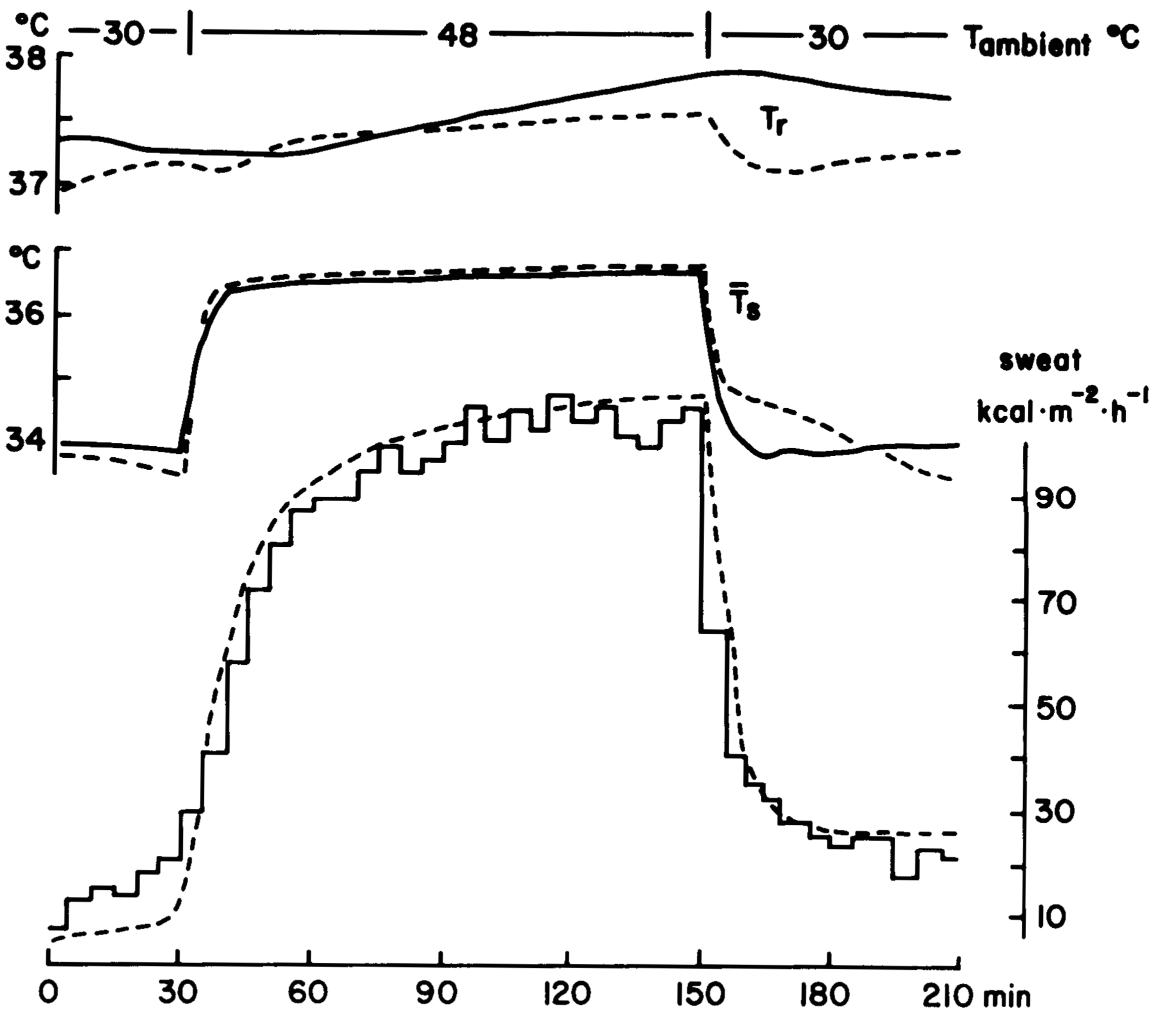

Figure 10. Experiment in which subject spends 30 minutes at thermally neutral temperature; 120 minutes at ambient temperature of 48° C; and 60 minutes recovery in 30° C environment.

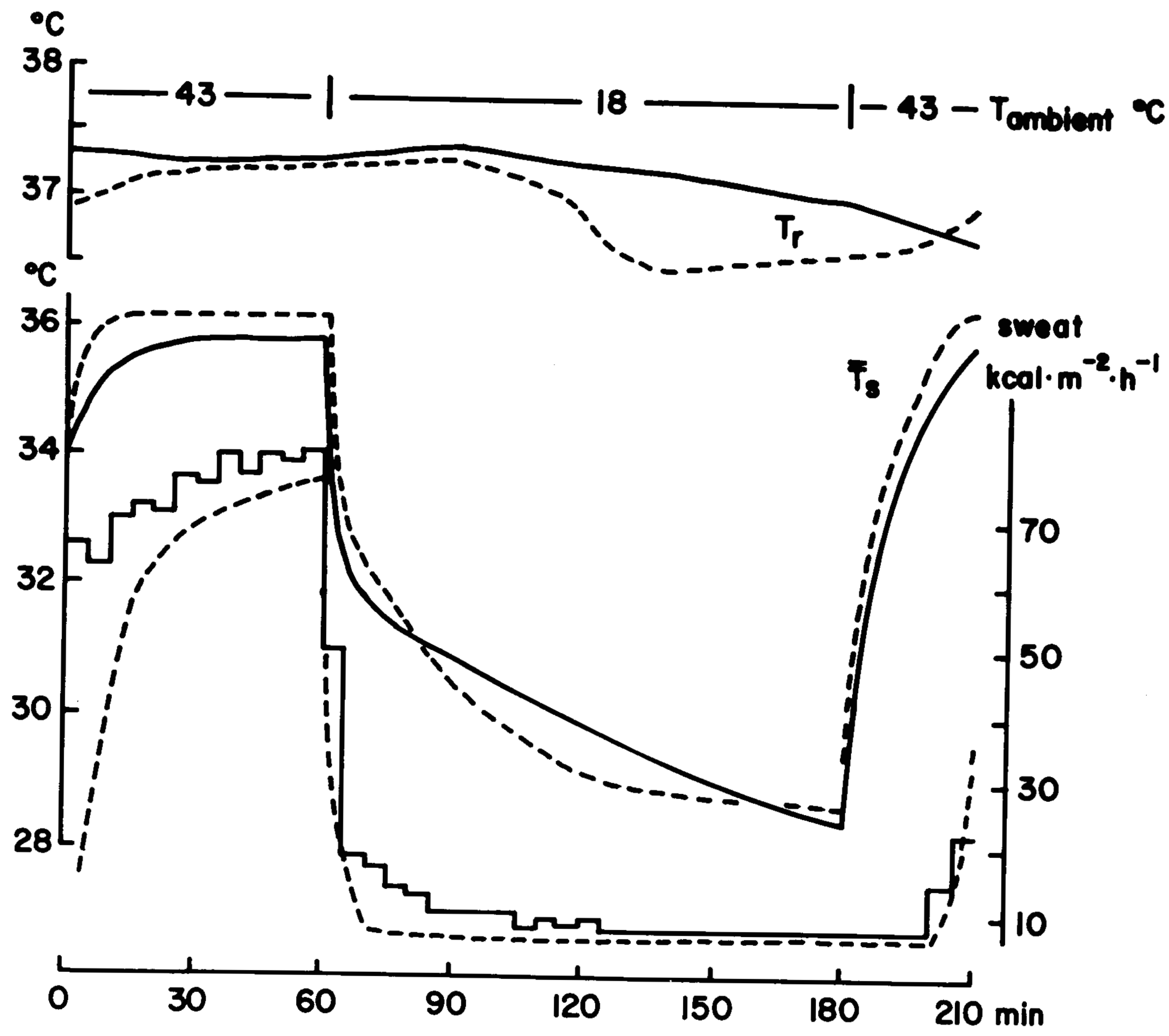

Figure 11. Experiment results

Table 15

TIME	S	M	EV	TB	TS	TH	TO	TR	TM	SBF	CO	COND	PWET
5	73.5	39.4	15.6	35.98	35.79	37.01	36.83	36.96	35.36	0.25	4.80	-34.9	10.0
10	45.9	39.4	40.9	36.15	36.13	37.13	36.92	37.07	35.52	0.53	5.08	-10.9	28.2
15	30.6	39.4	55.9	36.23	36.14	37.20	36.97	37.13	35.66	0.70	5.26	7.9	39.2
20	23.7	39.4	63.0	36.31	36.12	37.25	36.99	37.17	35.81	0.79	5.34	15.5	44.5
25	19.1	39.4	67.6	36.36	36.12	37.27	37.01	37.19	35.94	0.84	5.40	20.3	48.0
30	17.0	39.4	69.7	36.41	36.12	37.28	37.01	37.20	36.05	0.87	5.42	22.6	49.5
35	15.3	39.4	71.3	36.45	36.13	37.29	37.02	37.21	36.14	0.88	5.44	24.3	50.7
40	13.9	39.4	72.7	36.49	36.13	37.30	37.03	37.22	36.22	0.90	5.45	25.9	51.7
45	12.7	39.4	73.9	36.53	36.14	37.30	37.04	37.22	36.30	0.91	5.47	27.2	52.5
50	11.6	39.4	74.9	36.56	36.14	37.31	37.04	37.23	36.36	0.93	5.48	28.3	53.3
55	10.6	39.4	75.9	36.59	36.15	37.31	37.05	37.24	36.43	0.94	5.49	29.4	54.0
60	9.8	39.4	76.7	36.62	36.15	37.32	37.05	37.24	36.48	0.95	5.50	30.3	54.6
65	-89.3	39.4	20.8	36.34	33.59	37.30	37.03	37.23	36.45	0.21	4.76	36.4	9.1
70	-69.7	39.4	7.6	36.14	32.71	37.26	37.05	37.22	36.29	0.10	4.65	24.3	2.2
75	-64.7	39.4	7.4	35.96	31.99	37.26	37.09	37.25	36.08	0.05	4.61	19.7	2.2
80	-60.6	39.4	7.2	35.79	31.42	37.26	37.10	37.27	35.86	0.04	4.60	17.0	2.2
85	-57.2	39.4	7.1	35.64	30.98	37.24	37.08	37.27	35.64	0.04	4.59	15.2	2.2
90	-54.6	39.4	7.1	35.49	30.60	37.21	37.04	37.24	35.42	0.04	4.59	14.0	2.2
95	-52.3	39.4	7.0	35.34	30.28	37.16	37.00	37.20	35.22	0.03	4.59	13.1	2.2
100	-50.4	39.4	6.9	35.21	30.02	37.10	36.94	37.15	35.03	0.03	4.58	12.4	2.2
105	-47.5	40.6	6.9	35.07	29.76	37.03	36.86	37.08	34.84	0.03	4.62	11.9	2.2
110	-40.0	46.6	6.8	34.95	29.56	36.93	36.73	36.98	34.68	0.03	4.81	11.5	2.2
115	-29.3	56.0	6.8	34.86	29.40	36.79	36.57	36.84	34.55	0.03	5.10	11.4	2.2
120	-19.4	65.1	6.8	34.80	29.27	36.65	36.43	36.70	34.46	0.02	5.39	11.3	2.2
125	-9.6	74.1	6.7	34.77	29.17	36.54	36.34	36.58	34.38	0.02	5.67	11.1	2.2
130	-4.7	78.6	6.7	34.75	29.09	36.49	36.30	36.51	34.32	0.02	5.81	11.0	2.2
135	-2.7	80.2	6.7	34.74	29.03	36.47	36.30	36.49	34.26	0.02	5.86	10.9	2.2
140	-2.4	80.2	6.7	34.73	29.00	36.48	36.31	36.49	34.22	0.02	5.86	10.8	2.2
145	-2.9	79.5	6.7	34.72	28.96	36.49	36.32	36.50	34.17	0.02	5.84	10.7	2.2
150	-3.3	78.8	6.7	34.72	28.93	36.50	36.34	36.52	34.12	0.02	5.82	10.6	2.2
155	-3.8	78.1	6.7	34.71	28.90	36.52	36.35	36.53	34.08	0.02	5.79	10.5	2.2
160	-4.1	77.7	6.7	34.70	28.87	36.52	36.35	36.54	34.03	0.02	5.78	10.4	2.2
165	-4.1	77.5	6.7	34.68	28.84	36.53	36.36	36.54	33.98	0.02	5.77	10.3	2.2
170	-4.0	77.4	6.7	34.67	28.82	36.53	36.36	36.54	33.95	0.02	5.77	10.3	2.2
175	-3.9	77.4	6.7	34.66	28.80	36.53	36.36	36.54	33.91	0.02	5.77	10.2	2.2
180	-3.7	77.5	6.7	34.65	28.78	36.53	36.36	36.54	33.88	0.02	5.78	10.2	2.2
185	125.6	57.0	6.2	35.00	32.21	36.55	36.37	36.56	33.90	0.05	5.16	-17.0	4.3
190	102.8	46.4	6.6	35.31	33.86	36.62	36.42	36.59	34.06	0.08	4.85	-22.9	3.9
195	90.3	41.4	7.0	35.56	34.90	36.71	36.49	36.65	34.28	0.12	4.74	-32.0	3.8
200	82.4	39.7	7.3	35.79	35.74	36.81	36.58	36.73	34.53	0.20	4.76	-53.6	3.7
205	76.5	39.4	9.0	36.00	36.30	36.94	36.74	36.85	34.77	0.21	4.76	-90.4	4.6
210	47.4	39.4	37.6	36.16	36.35	37.10	36.88	37.00	35.01	0.48	5.03	-19.3	24.9

Performance of Model of Thermoregulation in Man During Exercise

In order to test the performance of the model in predicting the results of thermoregulatory stress resulting from internally produced heat during exercise, it was applied to conditions for which experimental measurements were obtained. Minimally dressed male subjects were seated on a bicycle ergometer, in an environment of 30°C at 30% relative humidity, with an air velocity of 10 cm . sec^{-1}. Evaporative heat loss was determined by weight recording, and metabolic rate through recording of oxygen consumption. Figure 12 shows the experimental results in solid lines, and the model predictions in broken lines. A more complete tabulation of the model responses is given in Table 16. This experiment constitutes a severe stress, and it requires well-trained individuals. Physically less fit subjects usually have to terminate the experiment before the end of the heavy exercise. During the final part of the heaviest exercise bout, the model estimates skin blood flow at over 3 liters . min^{-1}, and the percentage wetted area goes up to 66%, both these values are indices of thermal discomfort.

A comparison of an identical exercise experiment carried out at an ambient temperature of 20°C and the model prediction for the same condition is shown in Figure 13, with more complete model predictions in Table 17.

Discussion of Model Performance, Short Comings and the Path for Improvement

Any model is by definition simpler than the system it attempts to represent. The structure and definition of a model is focused on certain characteristics or conditions which are deemed of primary importance. In the manned space program, the thermophysiological problems are mainly related to prevention of hyperthermia (Stolwijk (41)). Both the experimental efforts and the emphasis of the model reported on here were directed at heat elimination. As can be seen in the previous section, the model predicts with reasonable accuracy the dynamic thermoregulatory responses to dynamic loads of ambient temperature and internal heat production even during very heavy exercise. There are discrepancies of absolute value and sometimes for short periods even of direction of change. Such discrepancies are associated with two types of conditions: exposure to thermal environments in which cooling occurs, and during the onset of exercise. During prolonged cooling, such as shown in Figure 11, between 60 and 180 minutes the core cools more in the simulation than in the experiment, and consequently shivering is initiated. The shivering causes perfusion of cold muscle with warm blood, and a resultant further drop of core temperatures increases shivering even more. Similarly in Figure 13 at 35 minutes and again at 95 minutes, there is a marked drop of core temperature at the onset of exercise, also due to perfusion of relatively cold muscle with warmer blood.

Since each of the segments in the controlled system consists of only 4 layers, there will be errors in the finite difference method of solution during the development of new gradients in the relatively thick muscle and core layers. During heat stress, such errors are small because the gradients are relatively small, and convective heat flow by the circulatory system is the major avenue of heat flow. During cooling this convective heat transport largely disappears, gradients appear and considerable errors can occur which tend to draw heat from the core in the model, before this happens in the experiment. Such errors tend to become smaller again as a steady state is approached. It is obvious that a simple remedy is available which consists of introducing additional layers in the controlled system. This method was used by Wissler (42) and it provides improved performance during cold exposure.

The erroneous, rapid and transient drop in internal temperature at the onset of exercise in the model, especially after prolonged rest in a cool environment, is probably the result of another simplification: immediately at the onset of exercise, the whole lumped mass of muscle in a given compartment is supplied with all the blood required for oxygen transport. Two factors are probably associated with the sudden drop in internal temperature. The present model does not make allowance for the development or repayment of an oxygen debt, and if such allowance were made it would tend to reduce the initial cooling of the blood in the muscle. A second factor might be that in a given muscle compartment not all muscles are likely to be active, so that those groups which are active warm up faster and cause less initial blood cooling than now occurs in the model.

Since it is intended to combine the present model of thermoregulation with simultaneous models of the cardio-vascular and the respiratory system, it is to be expected that improvements in this particular idiosyncrasy of the present thermoregulation model will result.

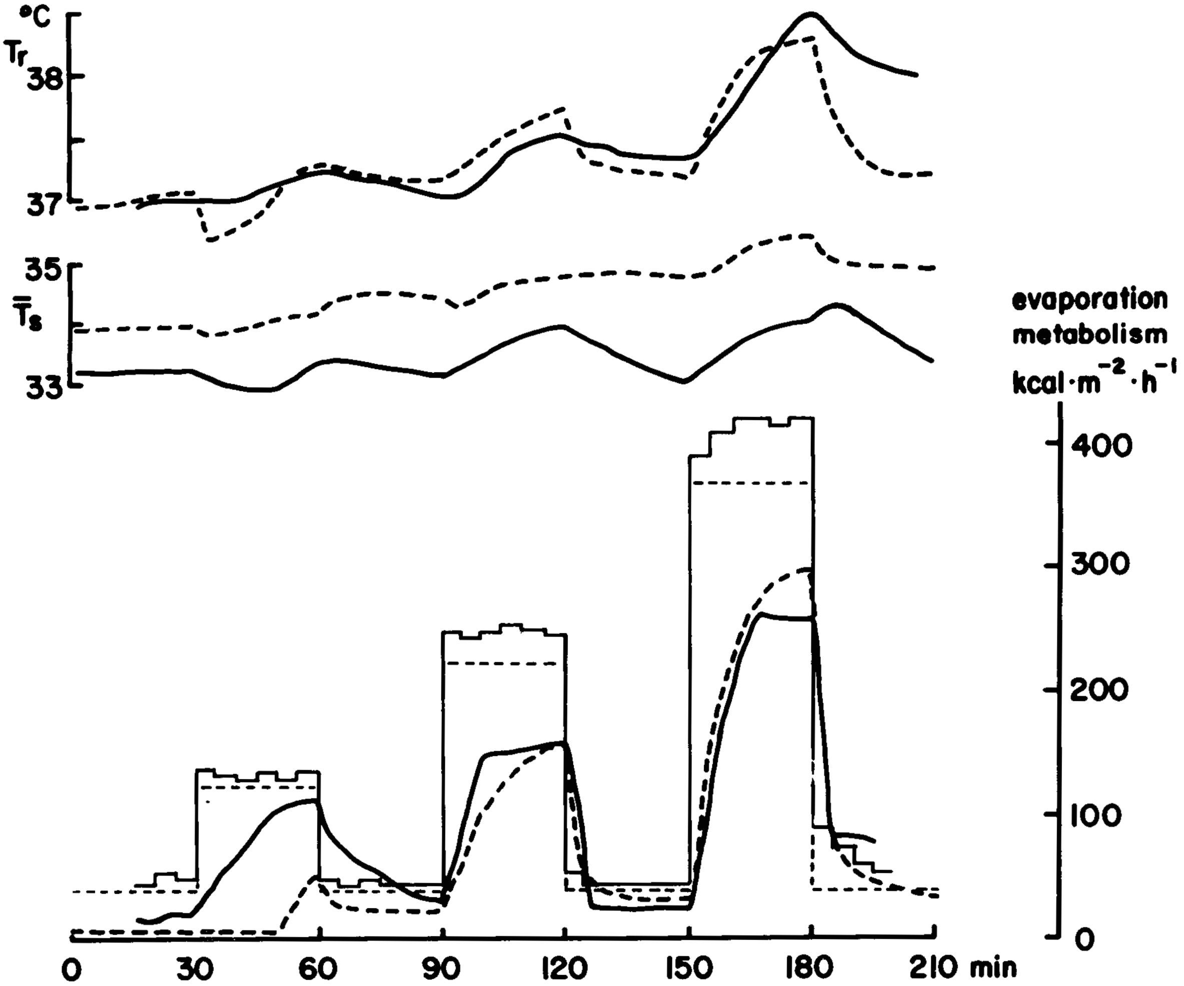

Figure 12. Experimental results.

Table 16

TIME	S	M	EV	TB	TS	TH	TO	TR	TM	SBF	CO	COND	PWET
5	5.1	40.1	7.6	35.76	33.97	36.98	36.78	36.94	35.30	0.11	4.68	11.3	2.6
10	4.8	39.8	7.6	35.78	33.97	37.02	36.81	36.97	35.31	0.11	4.67	11.1	2.6
15	4.5	39.5	7.6	35.79	33.97	37.05	36.85	37.01	35.31	0.11	4.66	11.0	2.6
20	4.4	39.4	7.6	35.80	33.97	37.08	36.88	37.04	35.32	0.11	4.66	10.9	2.6
25	4.4	39.4	7.6	35.81	33.97	37.11	36.90	37.07	35.33	0.11	4.66	10.9	2.6
30	4.1	39.4	7.6	35.82	34.00	37.12	36.90	37.08	35.34	0.13	4.69	11.0	2.6
35	74.6	127.7	14.3	36.01	33.81	36.77	36.49	36.67	36.48	0.09	7.42	16.1	1.1
40	73.5	127.3	14.3	36.24	33.90	36.83	36.69	36.73	37.00	0.09	7.41	15.7	1.1
45	70.2	125.3	14.3	36.40	34.00	36.97	36.86	36.88	37.23	0.10	7.36	15.7	1.1
50	67.5	124.3	14.8	36.59	34.15	37.17	37.04	37.08	37.46	0.15	7.37	16.2	1.3
55	43.9	124.3	37.5	36.73	34.21	37.28	37.12	37.20	37.62	0.35	7.58	24.3	7.4
60	31.3	124.3	49.6	36.83	34.25	37.34	37.16	37.26	37.71	0.48	7.70	28.5	10.6
65	-19.2	39.4	27.7	36.75	34.49	37.22	36.98	37.18	37.42	0.35	4.90	22.2	14.4
70	-17.3	39.4	25.3	36.71	34.54	37.21	36.97	37.17	37.24	0.33	4.89	22.0	13.0
75	-16.3	39.4	24.3	36.66	34.55	37.20	36.97	37.16	37.07	0.32	4.88	21.7	12.4
80	-15.4	39.4	23.5	36.62	34.53	37.19	36.96	37.15	36.95	0.32	4.87	21.3	11.9
85	-14.5	39.4	22.7	36.58	34.52	37.19	36.96	37.15	36.84	0.31	4.86	20.8	11.4
90	-13.6	39.4	22.0	36.54	34.50	37.19	36.95	37.14	36.75	0.30	4.85	20.3	11.0
95	120.7	223.5	58.0	36.92	34.39	37.34	37.29	37.20	37.85	0.52	10.86	29.3	10.7
100	76.4	223.5	100.2	37.17	34.60	37.56	37.44	37.41	38.16	1.13	11.47	45.5	21.7
105	49.0	223.5	126.4	37.34	34.70	37.70	37.54	37.54	38.30	1.43	11.78	55.1	28.4
110	33.9	223.5	140.9	37.45	34.76	37.79	37.60	37.63	38.39	1.60	11.95	60.4	32.1
115	23.0	223.5	151.5	37.53	34.79	37.84	37.64	37.68	38.44	1.73	12.07	64.3	34.7
120	16.5	223.5	157.7	37.57	34.81	37.87	37.66	37.70	38.47	1.80	12.15	66.6	36.3
125	-51.3	39.4	57.7	37.35	34.79	37.36	36.99	37.28	38.15	0.79	5.34	39.8	31.6
130	-33.0	39.4	38.9	37.23	34.86	37.24	36.99	37.19	37.88	0.56	5.12	32.6	20.5
135	-28.8	39.4	34.7	37.16	34.86	37.22	36.98	37.18	37.69	0.51	5.07	30.6	18.1
140	-26.7	39.4	32.7	37.09	34.84	37.21	36.97	37.17	37.53	0.49	5.05	29.5	17.0
145	-24.5	39.4	30.7	37.02	34.81	37.21	36.97	37.16	37.38	0.46	5.02	28.1	15.9
150	-23.0	39.4	29.5	36.96	34.77	37.20	36.96	37.16	37.26	0.44	4.99	27.0	15.2
155	168.3	370.2	152.2	37.56	34.87	37.80	37.89	37.58	38.63	1.59	16.55	57.2	31.7
160	91.8	370.2	226.4	37.88	35.10	38.18	38.11	37.93	38.94	2.47	17.43	82.5	50.2
165	51.0	370.2	265.8	38.07	35.22	38.37	38.22	38.11	39.08	2.93	17.89	96.5	59.7
170	31.4	370.2	284.7	38.17	35.29	38.47	38.28	38.20	39.15	3.15	18.11	103.4	64.2
175	22.4	370.2	293.1	38.24	35.36	38.53	38.32	38.25	39.20	3.29	18.25	107.4	65.8
180	17.1	370.2	297.9	38.30	35.41	38.56	38.35	38.29	39.23	3.38	18.34	110.4	66.6
185	-105.2	39.4	109.8	37.92	35.02	37.62	37.08	37.52	38.86	1.40	5.95	68.6	60.5
190	-53.4	39.4	58.3	37.74	35.00	37.35	37.04	37.29	38.56	0.78	5.34	44.0	31.4
195	-43.2	39.4	48.0	37.61	35.01	37.28	37.03	37.24	38.28	0.66	5.22	39.4	25.5
200	-38.1	39.4	43.2	37.51	34.98	37.26	37.02	37.22	38.08	0.61	5.16	36.6	22.8
205	-35.0	39.4	40.3	37.41	34.94	37.25	37.01	37.21	37.88	0.57	5.13	34.5	21.2
210	-32.3	39.4	37.9	37.32	34.90	37.24	37.00	37.20	37.71	0.55	5.10	32.7	19.9

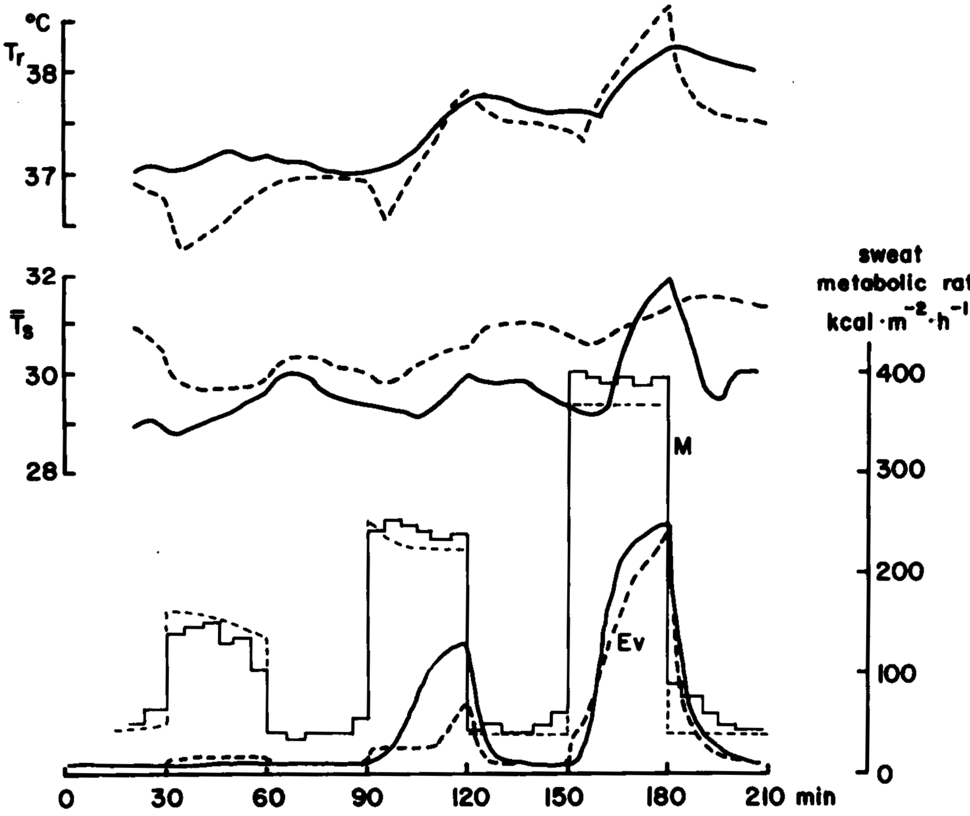

Figure 13. Experimental model prediction.

Table 17

TIME	S	M	EV	TB	TS	TH	TO	TR	TM	SBF	CO	COND	PWET
5	-51.9	41.9	7.4	35.60	32.48	36.97	36.76	36.93	35.26	0.06	4.69	21.1	2.2
10	-46.3	42.8	7.3	35.47	31.84	36.96	36.76	36.94	35.15	0.05	4.71	17.4	2.2
15	-40.9	44.7	7.2	35.34	31.36	36.92	36.72	36.92	35.01	0.04	4.76	15.3	2.2
20	-35.5	47.7	7.1	35.25	31.04	36.87	36.66	36.88	34.89	0.04	4.85	14.1	2.2
25	-29.7	51.6	7.0	35.16	30.76	36.80	36.59	36.81	34.77	0.04	4.97	13.3	2.2
30	-23.5	56.2	7.0	35.09	30.53	36.72	36.51	36.74	34.66	0.03	5.11	12.7	2.2
35	52.2	167.1	14.4	35.19	29.90	36.32	36.08	36.27	35.84	0.03	8.60	16.7	1.0
40	52.6	166.5	14.4	35.34	29.79	36.36	36.27	36.31	36.34	0.03	8.58	15.8	1.0
45	44.2	158.1	14.4	35.48	29.79	36.51	36.43	36.47	36.59	0.03	8.32	15.4	1.0
50	35.9	150.0	14.4	35.56	29.79	36.63	36.54	36.59	36.72	0.03	8.06	15.2	1.0
55	29.1	143.3	14.4	35.65	29.81	36.74	36.65	36.71	36.86	0.03	7.85	15.0	1.0
60	23.8	138.2	14.4	35.72	29.81	36.83	36.74	36.81	36.96	0.03	7.69	14.9	1.0
65	-27.9	50.1	7.0	35.65	30.31	36.86	36.75	36.91	36.46	0.03	4.92	11.5	2.2
70	-30.3	48.3	7.0	35.57	30.37	36.90	36.77	36.95	36.09	0.03	4.86	11.7	2.2
75	-30.8	47.5	7.0	35.49	30.33	36.91	36.78	36.96	35.84	0.03	4.84	11.6	2.2
80	-30.1	47.7	7.0	35.41	30.26	36.91	36.76	36.95	35.62	0.03	4.85	11.4	2.2
85	-28.4	48.8	6.9	35.33	30.18	36.89	36.74	36.93	35.43	0.03	4.88	11.2	2.2
90	-26.1	50.5	6.9	35.26	30.09	36.86	36.70	36.90	35.25	0.03	4.93	11.0	2.2
95	128.2	251.2	23.2	35.58	29.81	36.60	36.56	36.51	36.86	0.03	11.24	15.2	1.0
100	108.6	233.5	23.3	35.89	29.98	36.89	36.95	36.79	37.39	0.03	10.69	15.0	1.0
105	96.8	223.5	23.3	36.16	30.14	37.21	37.28	37.13	37.75	0.03	10.38	14.9	1.0
110	94.8	223.5	23.4	36.41	30.37	37.50	37.54	37.44	38.04	0.08	10.43	15.1	1.0
115	66.9	223.5	48.0	36.63	30.64	37.70	37.68	37.64	38.25	0.20	10.55	19.4	8.4
120	47.3	223.5	66.3	36.77	30.75	37.82	37.77	37.76	38.37	0.28	10.63	22.2	13.9
125	-58.0	39.4	19.5	36.59	31.30	37.51	37.28	37.54	37.83	0.16	4.71	15.6	10.2
130	-47.4	39.4	7.8	36.45	31.44	37.42	37.25	37.46	37.40	0.11	4.66	14.3	2.6
135	-46.5	39.4	7.2	36.32	31.38	37.39	37.23	37.43	37.07	0.09	4.64	14.1	2.2
140	-45.5	39.4	7.2	36.20	31.24	37.38	37.22	37.41	36.80	0.07	4.62	13.6	2.2
145	-44.3	39.4	7.2	36.08	31.08	37.37	37.22	37.41	36.55	0.06	4.61	13.0	2.2
150	-43.1	39.4	7.1	35.96	30.91	37.36	37.22	37.40	36.33	0.05	4.60	12.5	2.2
155	225.1	370.2	36.5	36.54	30.67	37.45	37.65	37.29	38.20	0.08	15.04	16.0	1.0
160	159.0	370.2	98.7	37.03	31.02	37.96	38.11	37.79	38.79	0.39	15.35	25.1	19.3
165	98.7	370.2	155.1	37.38	31.37	38.33	38.35	38.14	39.09	0.74	15.70	34.1	35.3
170	61.0	370.2	188.6	37.58	31.79	38.52	38.43	38.30	39.22	1.02	15.99	41.5	43.9
175	33.8	370.2	211.1	37.72	32.31	38.60	38.42	38.35	39.25	1.32	16.28	49.6	48.8
180	16.9	370.2	223.0	37.77	32.80	38.57	38.33	38.31	39.20	1.64	16.60	57.8	50.5
185	-102.8	39.4	50.2	37.37	32.42	37.66	37.26	37.59	38.70	0.38	4.94	28.7	31.7
190	-72.0	39.4	26.8	37.15	32.23	37.49	37.24	37.46	38.28	0.21	4.77	21.5	14.1
195	-62.3	39.4	18.2	36.96	32.08	37.44	37.24	37.44	37.90	0.16	4.72	19.0	8.8
200	-56.6	39.4	13.5	36.81	31.93	37.42	37.24	37.43	37.59	0.14	4.69	17.4	6.1
205	-52.2	39.4	10.1	36.67	31.80	37.41	37.23	37.42	37.32	0.12	4.67	16.2	4.0
210	-48.5	39.4	7.3	36.53	31.67	37.40	37.22	37.42	37.06	0.11	4.66	15.2	2.2

REFERENCES

1. Stolwijk, J. A. J. and J. D. Hardy, Temperature regulation in man - a theoretical study. Pflügers Arch. 291, 129-162 (1966).

2. Yamamoto, W. S. and W. F. Raub, Models of the regulation of internal respiration in mammals. Problems and promises. Computers and Biomet. Res. 1, 65-104 (1967).

3. Meeh, K., Oberflächenmessungen des menschlichen Körpers, J. Biol., 15, 428-458 (1879).

4. DuBois, D. and E. F. DuBois, Clinical Calorimetry: Fifth paper, The measurement of surface area of man. Arch. Intern. Med., 15, 868-888 (1915).

5. Bradfield, H. S., The determination of surface area of women and its use in expressing basal metabolic rate. Am. J. Physiol., 82, 570-576 (1927).

6. Wilmer, H. A., Changes in structural components of human body from six lunar months to maturity. Proc. Soc. Exp. Biol. Med., 43, 545-547 (1940).

7. Scammon, R. E., Developmental Anatomy In Schaeffer, J. P. (Editor) Morris' Human Anatomy, 11th Ed., New York, McGraw Hill (1953).

8. DuBois, D. and E. F. DuBois, Clinical Calorimetry: Tenth paper, A formula to estimate the approximate surface area if height and weight be known. Arch. Intern. Med., 17, 863-871 (1915).

REFERENCES

9. Nishi, Y. and A. P. Gagge, Mean skin temperature for man weighted by regional heat transfer coefficients. Fed. Proc. 29, 852 (1970).

10. Stolwijk, J. A. J. and J. D. Hardy. Partitional calorimetric studies of responses of man to thermal transients. J. Appl. Physiol., 21, 967-977 (1966).

11. Hardy, J. D. and J. A. J. Stolwijk, Partitional calorimetric studies of man during exposures to thermal transients. J. Appl. Physiol., 21, 1799-1806 (1966).

12. Brebner, D. F., D. McK. Kerslake and J. L. Waddell, The relation between the coefficients for heat exchange by convection and evaporation by man. J. Physiol., 141, 164-168 (1958).

13. Gagge, A. P., A new physiological variable associated with sensible and insensible perspiration. Am. J. Physiol., 120, 277-287 (1937).

14. Gagge, A. P., J. A. J. Stolwijk and B. Saltin, Comfort and thermal sensations and associated physiological responses during exercise at various ambient temperatures. Environmental Research, 2, 209-229 (1969).

15. Aschoff, Y. and R. Wever, Kern und Schale im Wärmehaushalt des Meuschen. Naturwinenschaften, 45, 477-485 (1958).

16. Scheinburg, P., L. I. Blackburn, M. Rich and M. Saslaw, Effects of vigorous physical exercise on cerebral circulation and metabolism. Am. J. Medicine, 16, 549-554 (1954).

REFERENCES

17. Behnke, A. R. and T. L. Willmon, Cutaneous diffusion of helium in relation to peripheral blood flow and absorption of atmospheric nitrogen through the skin. Am. J. Physiol., 131, 627-632 (1941).

18. Hertzman, A. B. and W. C. Randall, Regional differences in the basal and maximal rates of blood flow in the skin. J. Appl. Physiol., 1, 234-241 (1948)

19. Cabanac, M., J. A. J. Stolwijk and J. D. Hardy, Effect of temperature and pyrogens on single-unit activity in the rabbit's brain stem. J. Appl. Physiol., 24, 645-652 (1968).

20. Hellstrøm, B. and H. T. Hammel, Some characteristics of temperature regulation in unanesthetized dog. Am. J. Physiol., 213, 547-556 (1967)

21. Simon, E., W. Rautenberg, R. Thauer and M. Iriki, Die Auslösung von Kältezittern durch lokale Kühlung im Wirbelkanal. Pflügers Archiv., 281, 309-331 (1964).

22. Wünnenberg, W. and K. Brück, Untersuchimgen über die Funktionsweise thermoreceptiver Strukturen im Cervicalmark des Meerschweinchens. Pflügers Archiv., 294, 83 (1967).

23. Hensel, H., Electrophysiology of cutaneous thermoreceptors, In Skin senses, D. R. Kenshalo, Editor, Thomas, Springfield, Ill., (1968).

24. Bullard, R. W., M. R. Banerjee and B. A. MacIntyre, The role of the skin in negative feedback regulation of eccrine sweating. Int. J. Biometeor., 11, 93-104 (1967).

REFERENCES

25. Rawson, R. O. and K. P. Quick, Evidence of deep-body thermoreceptor response to intra-abdominal heating of the ewe. J. Appl. Physiol., 28, 813-820 (1970).

26. Wood, J. D., Electrical activity from single neurons in Auerbach's plexus. Am. J. Physiol., 219, 159-169 (1970).

27. Robinson, S., F. R. Meyer, J. L. Newton, C. H. TS'ao and L. O. Holgersen, Relations between sweating, cutaneous blood flow and body temperature in work. J. Appl. Physiol., 20, 575-582 (1965).

28. Bader, M. E. and M. B. Macht, Indirect peripheral vasodilatation produced by warming of various body areas. J. Appl. Physiol., 1, 215-226 (1948).

29. Randall, W. C., Quantitation and regional distribution of sweat glands in man. J. Clin. Invest., 25, 761-767 (1946).

30. Stolwijk, J. A. J., B. Saltin and A. P. Gagge, Physiological factors associated with sweating during exercise. J. Aerospace Med., 39, 1101-1105 (1968).

31. Bishop, J. M., K. W. Donald, S. H. Taylor and P. N. Wormald, Changes in arterial hepatic venous oxygen content difference during and after supine leg exercise. J. Physiol., 137, 309-317 (1957).

32. Bucht, H., J. Ek, H. Eliasch, A. Holmgren, B. Josephson and L. Werko, The effect of exercise in the recumbent position on the renal circulation and sodium excretion in normal individuals. Acta Physiol. Scand., 28, 95-100 (1953).

REFERENCES

33. Grimby, G. E., E. Haggendahl and B. Saltin, Local $Xenon^{133}$ clearance from the quadriceps muscle during exercise in man. J. Appl. Physiol., 22, 305-310 (1967).

34. Saltin, B., G. Blomquist, J. H. Mitchell, R. Johnson, Jr., K. Wildenthal and C. D. Chapman, Response to submaximal and maximal exercise after bed rest and training. Circulation, 38, Suppl. 7, 1-78 (1968).

35. Saltin, B., A. P. Gagge and J. A. J. Stolwijk, Muscle temperature during submaximal exercise in man. J. Appl. Physiol., 25, 679-688 (1968).

36. Webb-Peploe, M. M. and J. T. Shepherd. Peripheral mechanism involved in response of dogs' cutaneous veins to local temperature change. Circulation Res., 23, 701-708 (1968).

37. Wurster, R. D. and R. D. McCook, Influence of rate of change of skin temperature on sweating. J. Appl. Physiol. 27, 237-240 (1969).

38. Nadel, E. R., R. W. Bullard and J. A. J. Stolwijk, Sensitivity to rate of change in skin temperature in the regulation of sweating. m.s. to be submitted. (1970).

39. Benzinger, T. H., C. Kitzinger and A. W. Pratt, The Human Thermostat in Temperature - its measurement and control in science and industry, vol. 3, J. D. Hardy, Editor, p 637-665, Reinhold, New York (1963).

REFERENCES

40. Nadel, E. R., The role of peripheral thermoreceptors in the integrated thermoregulatory response in resting and exercising man. Dissertation, Univ. Calif., Santa Barbara (1969).

41. Stolwijk, J. A. J., Thermal loads in lunar ambulation. Aerospace Medicine (in press) (1970).

42. Wissler, E. H., A mathematical model of the human thermal system. Bull. Math. Biophysics, 26, 147-166 (1964).